

Exact Classical Quantum Mechanical Solution for Atomic Helium Which Predicts Conjugate Parameters from a Unique Solution for the First Time

Randell L. Mills, BlackLight Power, Inc., 493 Old Trenton Road, Cranbury, NJ 08512
(609)490-1090, rmills@blacklightpower.com, www.blacklightpower.com

Abstract

Quantum mechanics (QM) and quantum electrodynamics (QED) are often touted as the most successful theories ever. In this paper, this claim is critically evaluated by a test of internal consistency for the ability to calculate the conjugate observables of the nature of the free electron, ionization energy, elastic electron scattering, and the excited states of the helium atom using the same solution for each of the separate experimental measurements. It is found that in some cases quantum gives good numbers, but the solutions are meaningless numbers since each has no relationship to providing an accurate physical model. Rather, the goal is to mathematically reproduce an experimental or prior theoretical number using adjustable parameters including arbitrary wave functions in computer algorithms with precision that is often much greater (e.g. 8 significant figures greater) than possible based on the propagation of errors in the measured fundamental constants implicit in the physical problem. Given the constraints of adherence to physical laws and internal consistency, an extensive literature search indicates that quantum mechanics has never solved a single physical problem correctly including the hydrogen atom and the next member of the periodic chart, the helium atom. Rather than using postulated unverifiable theories that treat atomic particles as if they were not real, physical laws are now applied to the same problem. In an attempt to provide some physical insight into atomic problems and starting with the same essential physics as Bohr of e^- moving in the Coulombic field of the proton and the wave equation as modified after Schrödinger, a classical approach is explored which yields a model which is remarkably accurate and provides insight into physics on the atomic level. The proverbial view deeply seated in the wave-particle duality notion that there is no large-scale physical counterpart to the nature of the electron is shown not to be correct. Physical laws and intuition may be restored when dealing with the wave equation and quantum atomic problems. Specifically, a theory of classical quantum mechanics (CQM) was derived from first principles as reported previously [1-6] that successfully applies physical laws to the solution of atomic problems that has its basis in a breakthrough in the understanding of the stability of the bound electron to radiation. Rather than using the postulated Schrödinger boundary condition: " $\Psi \rightarrow 0$ as $r \rightarrow \infty$ ", which leads to a purely mathematical model of the electron, the constraint is based on experimental observation. Using Maxwell's equations, *the classical wave equation is solved with the constraint that the bound $n = 1$ -state electron cannot radiate energy.* Although it is well known that an accelerated *point* particle radiates, an *extended distribution* modeled as a superposition of accelerating charges does not have to radiate. A simple invariant physical model arises naturally wherein the predicted results are extremely straightforward and internally consistent requiring minimal math as in the case of the most famous equations of Newton, Maxwell, Einstein, de Broglie, and Planck on which the model is based. No new physics is needed; only the known physical laws based on direct observation are used. The accurate solution of the helium atom is confirmed by the agreement of predicted and observed conjugate parameters using the same unique physical model in all cases.

Key Words: theory, free electron, helium atom, ionization energy, elastic scattering, excited states, Maxwell's equations, conjugate parameters, internal consistency

Contents

I. Introduction

II. Classical Quantum Theory of the Atom Based on Maxwell's Equations

A. One-Electron Atoms

B. Spin Function

C. Angular Functions

D. Acceleration without Radiation

a. Special Relativistic Correction to the Electron Radius

b. Nonradiation Based on the Spacetime Fourier Transform of the Electron Current

c. Nonradiation Based on the Electron Electromagnetic Fields and the Poynting Power Vector

E. Magnetic Field Equations of the Electron

F. Stern-Gerlach Experiment

G. Electron g Factor

H. Spin and Orbital Parameters

a. Moment of Inertia and Spin and Rotational Energies

I. Force Balance Equation

J. Energy Calculations

K. Two Electron Atoms

a. Ionization Energies Calculated using the Poynting Power Theorem

III. Classical Scattering

A. Far Field Pattern

B. Two-Slit Interference (Wave-Particle Duality)

C. Electron Scattering from Helium

IV. Excited States of Helium

A. Singlet Excited States with $l = 0$ ($1s^2 \rightarrow 1s^1(ns^{\downarrow})$)

B. Triplet Excited States with $l = 0$ ($1s^2 \rightarrow 1s^1(ns^{\downarrow})$)

C. Singlet Excited States with $l \neq 0$

D. Triplet Excited States with $l \neq 0$

E. All Excited He I States

F. Spin-Orbital Coupling of Excited States with $l \neq 0$

V. Discussion

VI. Conclusion

References

I. Introduction

It is true that the Schrödinger equation can be solved exactly for the hydrogen atom; although, it is not true that the result is the exact solution of the hydrogen atom. Electron spin, the anomalous magnetic moment, the Lamb shift, fine structure, and hyperfine structure are missed entirely, and there are many internal inconsistencies and nonphysical consequences that do not agree with experimental results [1-9]. The Dirac equation does not reconcile this situation. Many additional shortcomings arise such as instability to radiation, negative kinetic energy states, intractable infinities, virtual particles at every point in space, self interaction, the Klein paradox, violation of Einstein causality, and "spooky" action at a distance [1, 7]. Despite its successes, quantum mechanics (QM) has remained mysterious to all who have encountered it. Starting with Bohr and progressing into the present, the departure from intuitive, physical reality has widened. The connection between quantum mechanics and reality is more than just a "philosophical" issue. It reveals that quantum mechanics is not a correct or complete theory of the physical world and that inescapable internal inconsistencies and incongruities arise when attempts are made to treat it as a physical as opposed to a purely mathematical "tool". Some of these issues are discussed in a review by Laloë [10].

But, QM has severe limitations even as a tool. Beyond one-electron atoms, multielectron-atom quantum mechanical equations can not be solved except by approximation methods [14] involving adjustable-parameter theories (perturbation theory, variational methods, self-consistent field method, multi-configuration Hartree Fock method, multi-configuration parametric potential method, $1/Z$ expansion method, multi-configuration Dirac-Fock method, electron correlation terms, QED terms, etc.)—all of which contain assumptions that can not be physically tested and are not consistent with physical laws.

Furthermore, unlike physical laws such as Maxwell's equations, it is always disconcerting to those that study quantum mechanics that it must be accepted without any underlying physical basis for fundamental observables such as the stability of the hydrogen atom in the first place. In this instance, a circular argument regarding definitions for parameters in the wave equation solutions and the Rydberg series of spectral lines replaces a first-principles-based prediction of those lines [1-9]. Nevertheless, it is felt that the application of the Schrödinger equation to real problems has provided useful approximations for physicists and chemists. Schrödinger interpreted $e\Psi^*(x)\Psi(x)$ as the charge-density or the amount of charge between x and $x + dx$ (Ψ^* is the complex conjugate of Ψ). Presumably, then, he pictured the electron to be spread over large regions of space. After Schrödinger's interpretation, Max Born, who was working with scattering theory, found that this interpretation led to inconsistencies, and he replaced the Schrödinger interpretation with the probability of finding the electron between x and $x + dx$ as

$$\int \Psi(x)\Psi^*(x)dx \tag{1}$$

Born's interpretation is generally accepted. Nonetheless, interpretation of the wave function is a never-ending source of confusion and conflict. Many scientists have solved this problem by conveniently adopting the Schrödinger interpretation for some problems and the Born interpretation for others. This duality allows the electron to be everywhere at one time—yet have no volume. Alternatively, the electron can be viewed as a discrete particle that moves here and there (from $r = 0$ to $r = \infty$), and $\Psi\Psi^*$ gives the time average of this motion.

Evidence that the point-particle probability-wave model of the electron is incorrect (i.e. it is not representative of reality) is that there is not a single example wherein a consistent set of calculations gives multiple conjugate observables. For example, the bound electron does not yield the accepted ionized electron in the limit that the bound electron is ionized. Consequently, a contradiction arises in the quantum mechanical scattering calculation. For hydrogen electron orbitals, the $n = \infty$ orbital is equivalent to an ionized electron. According to the quantum mechanical scattering model, the incident ionized electron is a plane wave. However, substitution of $n = \infty$ into the solution of the Schrödinger equation yields a radial function that has an infinite number of nodes and exists over all space. The hydrogen-like radial functions have $n - \ell - 1$ nodes between $r = 0$ and $r = \infty$. In fact, as $n \rightarrow \infty$ the Schrödinger equation becomes the equation of a linear harmonic oscillator [11]. The wavefunction shows sinusoidal behavior; thus, the wavefunction for the free electron can not be normalized and is infinite. In addition, the angular momentum of the free electron is infinite since it is given by $\ell(\ell+1)\hbar^2$ where $\ell \rightarrow \infty$. The results of the Davison-Germer experiment confirm that the ionized electron is a plane wave.

Bonham describes the method of calculating electron scattering from atoms according to quantum mechanics called the Born approximation that is an attempt at a physical model wherein a postulated plane wave electron scatters from the most probable structure for the atom. The Born approximation in the case of the He atom has the electrons and the nucleus collinear with the nucleus lying between the two electrons [12]. This is an average picture that is an ad hoc modification of the true model involving a three-point-body atom and a point-particle incident electron for which it is impossible to get neutral scattering. Rather, point-charge-like scattering given by the Rutherford equation is predicted. In the far field, the solution of the Schrödinger equation for the amplitude of the scattered plane wave incident on a three dimensional static potential field $U(r)$ can give a neutral-scattering pattern only if one assumes a continuous distribution of individual scattering points. This result is the basis of the failures of Schrödinger's interpretation that $\Psi(x)$ is the amplitude of the electron over three dimensional space in some sense and the superseding interpretation of the Born that $\Psi(x)$ represents a

probability function of a point electron. The Born interpretation can only be valid if the speed of the electron is equal to infinity. (The electron must be in all positions weighted by the probability density function during the time of the scattering event which is $< 10^{-17}$ s for a 500 eV electron scattered from helium). The Born interpretation must be rejected because the electron velocity can not exceed c without violating special relativity. Furthermore, even with Born's unjustified modification, the model fails utterly at predicting the experimental results at small scattering angles as reported previously [1, 13].

More recent calculations can achieve very good agreement with experimental results. Here, however the model is not physical; rather, it relies on totally arbitrary variational parameters that are adjusted in a trial-and-error manner until the correct behavior is obtained [15]. It is absolutely irrelevant whether the results match the data or not—any data including inaccurate data can be matched to infinite precision by such methods. The distinction between series expansion or variation of a physical parameter of an equation based on a physical action versus the fabrication of actions based on untestable constructs corresponding to a series with variational (adjustable) parameters is discussed elsewhere [6].

A third problem for the quantum mechanical model is that the helium wave equation used to calculate the scattering is not the Schrödinger equation solution for the ionization energy of the helium atom. Since it involves three bodies, the exact solution is impossible to be obtained. Many solutions have been obtained with great effort using various perturbation and adjustable-parameter methods as given by McQuarrie [14]. Such solutions are very dubious in that they are nonunique, not based on physical laws, and are better classified as curve fitting techniques in that they use up to 1000 adjustable parameters to obtain the ionization energy [14].

A fourth test of internal consistency regarding the helium atom is the ability to predict the ionization of two electron ions from the same equation as that of the helium atom. A further expectation is that additional multielectron atoms and ions may be solved from the two-electron atom solution due to linearity and superposition principles of electric and magnetic fields. Quantum mechanics fails miserably on both accounts. Quantum mechanical solutions other than the one-electron atom are obtained using unsubstantiated and ad hoc approximation methods such as the use of a perturbation series of postulated terms discussed *supra*. A fatal flaw is that these series diverge. These problems are discussed and the exact classical solutions are given in Refs. [1, 5].

In fact, even the Schrödinger equation results for one-electron atoms (the only problem that can be solved without approximations) are not accurate at all. It is nonrelativistic and there are major differences between predicted and experimental ionization energies as Z increases. It misses spin, the Lamb shift, the fine structure, and the hyperfine structure completely, it is not stable to radiation, and has many other problems with predictions that do not match

experimentation [1-9]. It also has an infinite number of solutions, not just the ones given in textbooks as given in Margenau and Murphy [16] and Ref. [8].

The Dirac equation is touted as remedying the nonrelativistic nature of the Schrödinger equation and providing an argument for the existence of virtual particles and corresponding so-called quantum electrodynamics (QED) computer algorithms for calculating unexpected observables such as the Lamb shift and the anomalous magnetic moment of the electron. But, both the Schrödinger and Dirac equations have many problems which make them untenable as representing reality as discussed *supra*.—infinities, lack of Einstein causality (spooky action at a distance), self interaction, instability to radiation, negative kinetic energy states, Klein paradox, and more [1-9]. This was argued by the founders of quantum mechanics [5]. Furthermore, QED is completely postulated. It involves a point electron which can not occupy any volume; consequently, all calculations have "intrinsic infinities" and require renormalization which is completely arbitrary. It further relies on a string of nonphysical constructs. For example, it is based on postulated polarization of the vacuum by postulated virtual particles which have no basis in reality, are fantastical at best, and conclusively shown to be impossible based on astrophysical observations [17]. Rather than invoking untestable "flights of fantasy", the results of QED such as the anomalous magnetic moment of the electron, the Lamb Shift, the fine structure and hyperfine structure of the hydrogen atom, and the hyperfine structure intervals of positronium and muonium can be solved exactly from Maxwell's equations to the limit possible based on experimental measurements which confirms QED's illegitimacy as representative of reality. These results and the implications to QED are reported and discussed in a companion paper [6].

A fifth test of internal consistency regarding the helium atom is the ability to predict the excited states from the "correct" helium-atom solution. Here quantum mechanics again fails, and in fact, offers no physical mechanism to yield excited states according to the Schrödinger equation since the calculation is based on the determination of the all-space integral involving continuous probability-density functions that ideally yields an energy minimum corresponding to the ground state [14]. No excited states exist in these methods. Thus, new mechanisms must be invented to mathematically generate numbers to match to the known helium excited states. For example, Duan et al. [18] claim to solve the Schrödinger equation for helium excited states. What they really do is take the known excited state energies and work backwards using a technique alien to quantum mechanics to find a wave equation that gives a node at a designated position as indicated the occurrence of eigenvalues that jump from negative to positive infinity and assign the node to the existence of a bound state, namely the one with the known trial energy. Specifically:

"For a given energy $E = -\varepsilon$, we can numerically calculate the matrix $F^{(S)\ell\lambda}(\rho)$ from equations (12, 13) by the method of analytical continuation. Namely, at a given position ρ and the length of step $\Delta\rho$ (say 0.1) we calculate $F^{(S)\ell\lambda}(\rho + \Delta\rho)$ by the Taylor series until the sum of the square elements of the next last term becomes less than 10^{-10} and that of the last term is smaller. If the term of $(\Delta\rho)^{22}$ could not satisfy this condition, we will decrease the length of the step. If the condition still could not be satisfied, it means a node appears and we calculate the inverse matrix $G^{(S)\ell\lambda}(\rho) = F^{(S)\ell\lambda}(\rho)^{-1}$ instead. We also check the eigenvalues of $F^{(S)\ell\lambda}(\rho)$ to see whether one of them becomes negative infinity (big number) and jumps to positive infinity and to make sure a node occurs. As ε decreases, if we find the number of nodes increases by one, it means a bound state occurs. The energy of the bound state is equal to $-\varepsilon$ where the additional node goes to infinity, and can be calculated by dichotomy."

Other techniques mentioned by Duan et al. [18] such as the hyperspherical harmonic (HH) method, the correlation HH method, the hyperspherical coordination method, the method of complex coordinate rotation, and the R-matrix method are ineffective and equally ad hoc. It can further be appreciated that these techniques are simply computer curve-fit algorithms since they often attempt to reproduce prior theoretical numbers using adjustable parameters including arbitrary wave functions in computer programs with precision that is often much greater than possible based on the propagation of errors in the measured fundamental constants implicit in the physical problem. Typically, the ionization energy and excited state levels can be determined spectroscopically to five to six significant figures, and calculations based on fundamental constants can be given to six-significant-figure accuracy based on the propagation of the experimental errors in the measured constants [19]. It is dubious that a precision of eight significant figures greater than that possible based on the limitations of the measured fundamental constants is reported in the literature [18].

As discussed herein, the success of quantum mechanics can be attributed to the use of arbitrary variational parameters in all-space probability wave functions and arbitrary renormalization of intrinsic infinities in the corresponding energies. With adjustable parameter methods, it is necessary to repeat trial-and-error experimentation to find which method of calculation gives the right answer. As is common practice McQuarrie [14], Brunger et al. [15], and B. Duan et al. [18] present only the successful procedure for the ionization energy, scattering, and excited states of helium as if it followed from first principles; and do not mention the actual method by which it was found. In electromagnetic theory based on Maxwell's equations, one deduces the computational algorithm from the general principles. In quantum theory as shown in the case of the determination of the conjugate parameters of the helium atom, the logic is just the opposite. One chooses the principle (e.g. phenomenological Hamiltonians) to fit the empirically successful algorithm and different internally inconsistent models are used

for different measurables such as ionization energy, scattering, and excited-state energies.

Thus, it can be argued that quantum mechanics gives correlations with experimental data. It does not explain the mechanism for the observed data. But, it should not be surprising that it may give good correlations given that the constraints of internal consistency and conformance to physical laws are removed for a wave equation with an infinite number of solutions wherein the solutions may be formulated as an infinite series of eigenfunctions with variable parameters. There are no physical constraints on the parameters. They may even correspond to unobservables such as virtual particles. If you invoke the constraints of internal consistency and conformance to physical laws, quantum mechanics has not successfully solved the physical problem of the one or two-electron atom.

In an attempt to provide some physical insight into atomic problems and starting with the same essential physics as Bohr of e^- moving in the Coulombic field of the proton and the wave equation as modified after Schrödinger, a classical approach was explored which yields a model which is remarkably accurate and provides insight into physics on the atomic level [1-6]. Physical laws and intuition are restored when dealing with the wave equation and quantum mechanical problems. Specifically, a theory of classical quantum mechanics (CQM) was derived from first principles that successfully applies physical laws on all scales. Rather than use the postulated Schrödinger boundary condition: " $\Psi \rightarrow 0$ as $r \rightarrow \infty$ ", which leads to a purely mathematical model of the electron, the constraint is based on experimental observation. Using Maxwell's equations, *the classical wave equation is solved with the constraint that the bound $n = 1$ -state electron cannot radiate energy.* The electron must be extended rather than a point. On this basis with the assumption that physical laws including Maxwell's equation apply to bound electrons, the hydrogen atom was solved exactly from first principles. The remarkable agreement across the spectrum of experimental results indicates that this is the correct model of the hydrogen atom.

It was shown previously that this approach gives a natural relationship between Maxwell's equations, special relativity, and general relativity. CQM holds over a scale of spacetime of 85 orders of magnitude—it correctly predicts the nature of the universe from the scale of the quarks to that of the cosmos. A review is given by Landvogt [20]. In another paper, the atomic physical approach was applied to multielectron atoms that were solved exactly disproving the deep-seated view that such exact solutions can not exist according to quantum mechanics. The general solutions for one through twenty-electron atoms are given in Ref [5]. The predictions are in remarkable agreement with the experimental values known for 400 atoms and ions. A further paper presents a solution based on physical laws and fully compliant with Maxwell's equations that solves the 26 parameters of molecular ions and molecules of hydrogen isotopes in closed-form equations with fundamental constants only that match the experimental

values. In a fifth paper of this series [6], rather than invoking renormalization, untestable virtual particles, and polarization of the vacuum by the virtual particles, the results of QED such as the anomalous magnetic moment of the electron, the Lamb Shift, the fine structure and hyperfine structure of the hydrogen atom, and the hyperfine structure intervals of positronium and muonium (thought to be only solvable using QED) are solved exactly from Maxwell's equations to the limit possible based on experimental measurements.

II. Classical Quantum Theory of the Atom Based on Maxwell's Equations

In this paper, the old view that the electron is a zero or one-dimensional point in an all-space probability wave function $\Psi(x)$ is not taken for granted. The theory of classical quantum mechanics (CQM), derived from first principles, must successfully and consistently apply physical laws on all scales [1-6]. Stability to radiation was ignored by all past atomic models. Historically, the point at which QM broke with classical laws can be traced to the issue of nonradiation of the one electron atom. Bohr just postulated orbits stable to radiation with the further postulate that the bound electron of the hydrogen atom does not obey Maxwell's equations—rather it obeys different physics [1-9]. Later physics was replaced by "pure mathematics" based on the notion of the inexplicable wave-particle duality nature of electrons which lead to the Schrödinger equation wherein the consequences of radiation predicted by Maxwell's equations were ignored. Ironically, Bohr, Schrödinger, and Dirac used the Coulomb potential, and Dirac used the vector potential of Maxwell's equations. But, all ignored electrodynamics and the corresponding radiative consequences. Dirac originally attempted to solve the bound electron physically with stability with respect to radiation according to Maxwell's equations with the further constraints that it was relativistically invariant and gave rise to electron spin [21]. He and many founders of QM such as Sommerfeld, Bohm, and Weinstein wrongly pursued a planetary model, were unsuccessful, and resorted to the current mathematical-probability-wave model that has many problems [1-9, 21-24]. Consequently, Feynman for example, attempted to use first principles including Maxwell's equations to discover new physics to replace quantum mechanics [25].

Physical laws may indeed be the root of the observations thought to be "purely quantum mechanical", and it may have been a mistake to make the assumption that Maxwell's electrodynamic equations must be rejected at the atomic level. Thus, in the present approach, the classical wave equation is solved with the constraint that a bound $n = 1$ -state electron cannot radiate energy.

Herein, derivations consider the electrodynamic effects of moving charges as well as the Coulomb potential, and the search is for a solution representative of the electron wherein there is acceleration of charge motion without radiation. The mathematical formulation for zero

radiation based on Maxwell's equations follows from a derivation by Haus [26]. The function that describes the motion of the electron must not possess spacetime Fourier components that are synchronous with waves traveling at the speed of light. Similarly, nonradiation is demonstrated based on the electron's electromagnetic fields and the Poynting power vector.

It was shown previously [1-6] that CQM gives closed form solutions for the atom including the stability of the $n = 1$ state and the instability of the excited states, the equation of the photon and electron in excited states, the equation of the free electron, and photon which predict the wave particle duality behavior of particles and light. The current and charge density functions of the electron may be directly physically interpreted. For example, spin angular momentum results from the motion of negatively charged mass moving systematically, and the equation for angular momentum, $\mathbf{r} \times \mathbf{p}$, can be applied directly to the wave function (a current density function) that describes the electron. The magnetic moment of a Bohr magneton, Stern Gerlach experiment, g factor, Lamb shift, resonant line width and shape, selection rules, correspondence principle, wave particle duality, excited states, reduced mass, rotational energies, and momenta, orbital and spin splitting, spin-orbital coupling, Knight shift, and spin-nuclear coupling, and elastic electron scattering from helium atoms, are derived in closed form equations based on Maxwell's equations. The calculations agree with experimental observations.

In contrast to the failure of the Bohr theory and the nonphysical, adjustable-parameter approach of quantum mechanics, multielectron atoms [1, 5] and the nature of the chemical bond [1, 4] are given by exact closed-form solutions containing fundamental constants only. Using the nonradiative wave equation solutions that describe the bound electron having conserved momentum and energy, the radii are determined from the force balance of the electric, magnetic, and centrifugal forces that corresponds to the minimum of energy of the system. The ionization energies are then given by the electric and magnetic energies at these radii. The spreadsheets to calculate the energies from exact solutions of one through twenty-electron atoms are available from the internet [27]. For 400 atoms and ions the agreement between the predicted and experimental results is remarkable.

A. One-Electron Atoms

One-electron atoms include the hydrogen atom, He^+ , Li^{2+} , Be^{3+} , and so on. The mass-energy and angular momentum of the electron are constant; this requires that the equation of motion of the electron be temporally and spatially harmonic. Thus, the classical wave equation applies and

$$\left[\nabla^2 - \frac{1}{v^2} \frac{\partial^2}{\partial t^2} \right] \rho(r, \theta, \phi, t) = 0 \quad (2)$$

where $\rho(r, \theta, \phi, t)$ is the time dependent charge density function of the electron in time and

space. In general, the wave equation has an infinite number of solutions. To arrive at the solution which represents the electron, a suitable boundary condition must be imposed. It is well known from experiments that each single atomic electron of a given isotope radiates to the same stable state. Thus, the physical boundary condition of nonradiation of the bound electron was imposed on the solution of the wave equation for the time dependent charge density function of the electron [1-3, 5]. The condition for radiation by a moving point charge given by Haus [26] is that its spacetime Fourier transform does possess components that are synchronous with waves traveling at the speed of light. Conversely, it is proposed that the condition for nonradiation by an ensemble of moving point charges that comprises a current density function is

For non-radiative states, the current-density function must NOT possess spacetime Fourier components that are synchronous with waves traveling at the speed of light.

The time, radial, and angular solutions of the wave equation are separable. The motion is time harmonic with frequency ω_n . A constant angular function is a solution to the wave equation. Solutions of the Schrödinger wave equation comprising a radial function radiate according to Maxwell's equation as shown previously by application of Haus' condition [1]. In fact, it was found that any function which permitted radial motion gave rise to radiation. A radial function which does satisfy the boundary condition is a radial delta function

$$f(r) = \frac{1}{r^2} \delta(r - r_n) \quad (3)$$

This function defines a constant charge density on a spherical shell where $r_n = nr_1$ wherein n is an integer in an excited state, and Eq. (2) becomes the two-dimensional wave equation plus time with separable time and angular functions. Given time harmonic motion and a radial delta function, the relationship between an allowed radius and the electron wavelength is given by

$$2\pi r_n = \lambda_n \quad (4)$$

where the integer subscript n here and in Eq. (3) is determined during photon absorption as given in the Excited States of the One-Electron Atom (Quantization) section of Ref. [1]. Using the observed de Broglie relationship for the electron mass where the coordinates are spherical,

$$\lambda_n = \frac{h}{p_n} = \frac{h}{m_e v_n} \quad (5)$$

and the magnitude of the velocity for every point on the orbitsphere is

$$v_n = \frac{\hbar}{m_e r_n} \quad (6)$$

The sum of the $|\mathbf{L}_i|$, the magnitude of the angular momentum of each infinitesimal point of the orbitsphere of mass m_i , must be constant. The constant is \hbar .

$$\sum |\mathbf{L}_i| = \sum |\mathbf{r} \times m_i \mathbf{v}| = m_e r_n \frac{\hbar}{m_e r_n} = \hbar \quad (7)$$

Thus, an electron is a spinning, two-dimensional spherical surface (zero thickness), called an *electron orbitsphere* shown in Figure 1, that can exist in a bound state at only specified distances from the nucleus determined by an energy minimum. The corresponding current function shown in Figure 2 which gives rise to the phenomenon of *spin* is derived in the Spin Function section. (See the Orbitsphere Equation of Motion for $\ell = 0$ of Ref. [1] at Chp. 1.)

Nonconstant functions are also solutions for the angular functions. To be a harmonic solution of the wave equation in spherical coordinates, these angular functions must be spherical harmonic functions [28]. A zero of the spacetime Fourier transform of the product function of two spherical harmonic angular functions, a time harmonic function, and an unknown radial function is sought. The solution for the radial function which satisfies the boundary condition is also a delta function given by Eq. (3). Thus, bound electrons are described by a charge-density (mass-density) function which is the product of a radial delta function, two angular functions (spherical harmonic functions), and a time harmonic function.

$$\rho(r, \theta, \phi, t) = f(r)A(\theta, \phi, t) = \frac{1}{r^2} \delta(r - r_n)A(\theta, \phi, t); \quad A(\theta, \phi, t) = Y(\theta, \phi)k(t) \quad (8)$$

In these cases, the spherical harmonic functions correspond to a traveling charge density wave confined to the spherical shell which gives rise to the phenomenon of orbital angular momentum. The orbital functions which modulate the constant "spin" function shown graphically in Figure 3 are given in the Sec. IIC.

B. Spin Function

The orbitsphere spin function comprises a constant charge (current) density function with moving charge confined to a two-dimensional spherical shell. The magnetostatic current pattern of the orbitsphere spin function comprises an infinite series of correlated orthogonal great circle current loops wherein each point charge (current) density element moves time harmonically with constant angular velocity

$$\omega_n = \frac{\hbar}{m_e r_n^2} \quad (9)$$

The uniform current density function $Y_0^0(\phi, \theta)$, the orbitsphere equation of motion of the electron (Eqs. (14-15)), corresponding to the constant charge function of the orbitsphere that gives rise to the spin of the electron is generated from a basis set current-vector field defined as the orbitsphere current-vector field ("orbitsphere-cvf"). This in turn is generated over the surface by two complementary steps of an infinite series of nested rotations of two orthogonal great circle current loops where the coordinate axes rotate with the two orthogonal great circles that

serve as a basis set. The algorithm to generate the current density function rotates the great circles and the corresponding x'y'z' coordinates relative to the xyz frame. Each infinitesimal rotation of the infinite series is about the new i'-axis and new j'-axis which results from the preceding such rotation. Each element of the current density function is obtained with each conjugate set of rotations. In Appendix III of Ref. [1], the *continuous* uniform electron current density function $Y_0^0(\phi, \theta)$ having the same angular momentum components as that of the orbitosphere-cvf is then exactly generated from this orbitosphere-cvf as a basis element by a convolution operator comprising an autocorrelation-type function.

For Step One, the current density elements move counter clockwise on the great circle in the y'z'-plane and move clockwise on the great circle in the x'z'-plane. The great circles are rotated by an infinitesimal angle $\pm\Delta\alpha_i$ (a positive rotation around the x'-axis or a negative rotation about the z'-axis for Steps One and Two, respectively) and then by $\pm\Delta\alpha_j$ (a positive rotation around the new y'-axis or a positive rotation about the new x'-axis for Steps One and Two, respectively). The coordinates of each point on each rotated great circle (x',y',z') is expressed in terms of the first (x,y,z) coordinates by the following transforms where clockwise rotations and motions are defined as positive looking along the corresponding axis:

Step One

$$\begin{bmatrix} x \\ y \\ z \end{bmatrix} = \begin{bmatrix} \cos(\Delta\alpha_y) & 0 & -\sin(\Delta\alpha_y) \\ 0 & 1 & 0 \\ \sin(\Delta\alpha_y) & 0 & \cos(\Delta\alpha_y) \end{bmatrix} \begin{bmatrix} 1 & 0 & 0 \\ 0 & \cos(\Delta\alpha_x) & \sin(\Delta\alpha_x) \\ 0 & -\sin(\Delta\alpha_x) & \cos(\Delta\alpha_x) \end{bmatrix} \begin{bmatrix} x' \\ y' \\ z' \end{bmatrix}$$

$$\begin{bmatrix} x \\ y \\ z \end{bmatrix} = \begin{bmatrix} \cos(\Delta\alpha_y) & \sin(\Delta\alpha_y)\sin(\Delta\alpha_x) & -\sin(\Delta\alpha_y)\cos(\Delta\alpha_x) \\ 0 & \cos(\Delta\alpha_x) & \sin(\Delta\alpha_x) \\ \sin(\Delta\alpha_y) & -\cos(\Delta\alpha_y)\sin(\Delta\alpha_x) & \cos(\Delta\alpha_y)\cos(\Delta\alpha_x) \end{bmatrix} \begin{bmatrix} x' \\ y' \\ z' \end{bmatrix}$$

(10)

Step Two

$$\begin{bmatrix} x \\ y \\ z \end{bmatrix} = \begin{bmatrix} 1 & 0 & 0 \\ 0 & \cos(\Delta\alpha_x) & \sin(\Delta\alpha_x) \\ 0 & -\sin(\Delta\alpha_x) & \cos(\Delta\alpha_x) \end{bmatrix} \begin{bmatrix} \cos(\Delta\alpha_z) & \sin(\Delta\alpha_z) & 0 \\ -\sin(\Delta\alpha_z) & \cos(\Delta\alpha_z) & 0 \\ 0 & 0 & 1 \end{bmatrix} \begin{bmatrix} x' \\ y' \\ z' \end{bmatrix}$$

$$\begin{bmatrix} x \\ y \\ z \end{bmatrix} = \begin{bmatrix} \cos(\Delta\alpha_z) & \sin(\Delta\alpha_z) & 0 \\ -\cos(\Delta\alpha_x)\sin(\Delta\alpha_z) & \cos(\Delta\alpha_x)\cos(\Delta\alpha_z) & \sin(\Delta\alpha_x) \\ \sin(\Delta\alpha_x)\sin(\Delta\alpha_z) & -\sin(\Delta\alpha_x)\cos(\Delta\alpha_z) & \cos(\Delta\alpha_x) \end{bmatrix} \begin{bmatrix} x' \\ y' \\ z' \end{bmatrix}$$

(11)

where the angular sum is $\lim_{\Delta\alpha \rightarrow 0} \sum_{n=1}^{\frac{\sqrt{2}}{2}\pi} |\Delta\alpha_{i,j}| = \frac{\sqrt{2}}{2}\pi$.

The orbitsphere-cvf is given by n reiterations of Eqs. (10) and (11) for each point on each of the two orthogonal great circles during each of Steps One and Two. The output given by the non-primed coordinates is the input of the next iteration corresponding to each successive nested rotation by the infinitesimal angle $\pm\Delta\alpha_i$ or $\pm\Delta\alpha_j$, where the magnitude of the angular sum of the n rotations about each of the i'-axis and the j'-axis is $\frac{\sqrt{2}}{2}\pi$. Half of the orbitsphere-cvf is generated during each of Steps One and Two.

Following Step Two, in order to match the boundary condition that the magnitude of the velocity at any given point on the surface is given by Eq. (6), the output half of the orbitsphere-cvf is rotated clockwise by an angle of $\frac{\pi}{4}$ about the z-axis. Using Eq. (11) with $\Delta\alpha_z = \frac{\pi}{4}$ and $\Delta\alpha_x = 0$ gives the rotation. Then, the one half of the orbitsphere-cvf generated from Step One is superimposed with the complementary half obtained from Step Two following its rotation about the z-axis of $\frac{\pi}{4}$ to give the basis function to generate $Y_0^0(\phi, \theta)$, the orbitsphere equation of motion of the electron.

The current pattern of the orbitsphere-cvf generated by the nested rotations of the orthogonal great circle current loops is a continuous and total coverage of the spherical surface, but it is shown as a visual representation using 6 degree increments of the infinitesimal angular variable $\pm\Delta\alpha_i$ and $\pm\Delta\alpha_j$, of Eqs. (10) and (11) from the perspective of the z-axis in Figure 2.

In each case, the complete orbitsphere-cvf current pattern corresponds all the orthogonal-great-circle elements which are generated by the rotation of the basis-set according to Eqs. (10) and (11) where $\pm\Delta\alpha_i$ and $\pm\Delta\alpha_j$ approach zero and the summation of the infinitesimal angular rotations of $\pm\Delta\alpha_i$ and $\pm\Delta\alpha_j$ about the successive i'-axes and j'-axes is $\frac{\sqrt{2}}{2}\pi$ for each Step.

The current pattern gives rise to the phenomenon corresponding to the spin quantum number. The details of the derivation of the spin function are given in Ref. [3] and Chp. 1 of Ref. [1].

The resultant angular momentum projections of $\mathbf{L}_{xy} = \frac{\hbar}{4}$ and $\mathbf{L}_z = \frac{\hbar}{2}$ meet the boundary condition for the unique current having an angular velocity magnitude at each point on the surface given by Eq. (6) and give rise to the Stern Gerlach experiment as shown in Ref. [1]. The further constraint that the current density is uniform such that the charge density is uniform, corresponding to an equipotential, minimum energy surface is satisfied by using the orbitsphere-cvf as a basis element to generate $Y_0^0(\phi, \theta)$ using a convolution operator comprising an autocorrelation-type function as given in Appendix III of Ref. [1]. The operator comprises the convolution of each great circle current loop of the orbitsphere-cvf designated as the primary orbitsphere-cvf with a second orbitsphere-cvf designated as the secondary orbitsphere-cvf wherein the convolved secondary elements are matched for orientation, angular momentum, and phase to those of the primary. The resulting exact uniform current distribution obtained from the convolution has the same angular momentum distribution, resultant, \mathbf{L}_R , and components of $\mathbf{L}_{xy} = \frac{\hbar}{4}$ and $\mathbf{L}_z = \frac{\hbar}{2}$ as those of the orbitsphere-cvf used as a primary basis element.

C. Angular Functions

The time, radial, and angular solutions of the wave equation are separable. Also based on the radial solution, the angular charge and current-density functions of the electron, $A(\theta, \phi, t)$, must be a solution of the wave equation in two dimensions (plus time),

$$\left[\nabla^2 - \frac{1}{v^2} \frac{\partial^2}{\partial t^2} \right] A(\theta, \phi, t) = 0 \quad (12)$$

where $\rho(r, \theta, \phi, t) = f(r)A(\theta, \phi, t) = \frac{1}{r^2} \delta(r - r_n)A(\theta, \phi, t)$ and $A(\theta, \phi, t) = Y(\theta, \phi)k(t)$

$$\left[\frac{1}{r^2 \sin \theta} \frac{\partial}{\partial \theta} \left(\sin \theta \frac{\partial}{\partial \theta} \right)_{r, \phi} + \frac{1}{r^2 \sin^2 \theta} \left(\frac{\partial^2}{\partial \phi^2} \right)_{r, \theta} - \frac{1}{v^2} \frac{\partial^2}{\partial t^2} \right] A(\theta, \phi, t) = 0 \quad (13)$$

where v is the linear velocity of the electron. The charge-density functions including the time-function factor are

$$\mathfrak{L} = 0$$

$$\rho(r, \theta, \phi, t) = \frac{e}{8\pi r^2} [\delta(r - r_n)] [Y_0^0(\theta, \phi) + Y_\ell^m(\theta, \phi)] \quad (14)$$

$\ell \neq 0$

$$\rho(r, \theta, \phi, t) = \frac{e}{4\pi r^2} [\delta(r - r_n)] [Y_0^0(\theta, \phi) + \text{Re}\{Y_\ell^m(\theta, \phi)e^{i\omega_n t}\}] \quad (15)$$

where $Y_\ell^m(\theta, \phi)$ are the spherical harmonic functions that spin about the z-axis with angular frequency ω_n with $Y_0^0(\theta, \phi)$ the constant function. $\text{Re}\{Y_\ell^m(\theta, \phi)e^{i\omega_n t}\} = P_\ell^m(\cos\theta)\cos(m\phi + \omega_n t)$ where to keep the form of the spherical harmonic as a traveling wave about the z-axis, $\omega_n = m\omega_n$.

D. Acceleration without Radiation

a. Special Relativistic Correction to the Electron Radius

The relationship between the electron wavelength and its radius is given by Eq. (4) where λ is the de Broglie wavelength. For each current density element of the spin function, the distance along each great circle in the direction of instantaneous motion undergoes length contraction and time dilation. Using a phase matching condition, the wavelengths of the electron and laboratory inertial frames are equated, and the corrected radius is given by

$$r_n = r_n' \left[\sqrt{1 - \left(\frac{v}{c}\right)^2} \sin \left[\frac{\pi}{2} \left(1 - \left(\frac{v}{c}\right)^2\right)^{3/2} \right] + \frac{1}{2\pi} \cos \left[\frac{\pi}{2} \left(1 - \left(\frac{v}{c}\right)^2\right)^{3/2} \right] \right] \quad (16)$$

where the electron velocity is given by Eq. (6). (See Ref. [1] Chp. 1, Special Relativistic Correction to the Ionization Energies section). $\frac{e}{m_e}$ of the electron, the electron angular momentum of \hbar , and μ_B are invariant, but the mass and charge densities increase in the laboratory frame due to the relativistically contracted electron radius. As $v \rightarrow c$, $r/r' \rightarrow \frac{1}{2\pi}$ and $r = \lambda$ as shown in Figure 4.

b. Nonradiation Based on the Spacetime Fourier Transform of the Electron Current

The Fourier transform of the electron charge density function given by Eq. (8) is a solution of the three-dimensional wave equation in frequency space (\mathbf{k}, ω space) as given in Chp 1, Spacetime Fourier Transform of the Electron Function section of Ref. [1]. Then the corresponding Fourier transform of the current density function $K(s, \Theta, \Phi, \omega)$ is given by

multiplying by the constant angular frequency.

$$\begin{aligned}
K(s, \Theta, \Phi, \omega) &= 4\pi\omega_n \frac{\sin(2s_n r_n)}{2s_n r_n} \otimes 2\pi \sum_{\nu=1}^{\infty} \frac{(-1)^{\nu-1} (\pi \sin \Theta)^{2(\nu-1)}}{(\nu-1)!(\nu-1)!} \frac{\Gamma\left(\frac{1}{2}\right)\Gamma\left(\nu+\frac{1}{2}\right)}{(\pi \cos \Theta)^{2\nu+1} 2^{\nu+1}} \frac{2\nu!}{(\nu-1)!} s^{-2\nu} \\
&\otimes 2\pi \sum_{\nu=1}^{\infty} \frac{(-1)^{\nu-1} (\pi \sin \Phi)^{2(\nu-1)}}{(\nu-1)!(\nu-1)!} \frac{\Gamma\left(\frac{1}{2}\right)\Gamma\left(\nu+\frac{1}{2}\right)}{(\pi \cos \Phi)^{2\nu+1} 2^{\nu+1}} \frac{2\nu!}{(\nu-1)!} s^{-2\nu} \frac{1}{4\pi} [\delta(\omega - \omega_n) + \delta(\omega + \omega_n)]
\end{aligned} \tag{17}$$

$\mathbf{s}_n \cdot \mathbf{v}_n = \mathbf{s}_n \cdot \mathbf{c} = \omega_n$ implies $r_n = \lambda_n$ which is given by Eq. (16) in the case that k is the lightlike k^0 . In this case, Eq. (17) vanishes. Consequently, spacetime harmonics of $\frac{\omega_n}{c} = k$ or $\frac{\omega_n}{c} \sqrt{\frac{\epsilon}{\epsilon_0}} = k$ for which the Fourier transform of the current-density function is nonzero do not

exist. Radiation due to charge motion does not occur in any medium when this boundary condition is met. Nonradiation is also determined directly from the fields based on Maxwell's equations as given in Sec. IIDc.

c. Nonradiation Based on the Electron Electromagnetic Fields and the Poynting Power Vector

A point charge undergoing periodic motion accelerates and as a consequence radiates according to the Larmor formula:

$$P = \frac{1}{4\pi\epsilon_0} \frac{2e^2}{3c^3} a^2 \tag{18}$$

where e is the charge, a is its acceleration, ϵ_0 is the permittivity of free space, and c is the speed of light. Although an accelerated *point* particle radiates, an *extended distribution* modeled as a superposition of accelerating charges does not have to radiate [21, 26, 29-31]. In Ref. [3] and Appendix I, Chp. 1 of Ref. [1], the electromagnetic far field is determined from the current distribution in order to obtain the condition, if it exists, that the electron current distribution must satisfy such that the electron does not radiate. The current follows from Eqs. (14-15). The currents corresponding to Eq. (14) and first term of Eq. (15) are static. Thus, they are trivially nonradiative. The current due to the time dependent term of Eq. (15) corresponding to p, d, f, etc. orbitals is

$$\begin{aligned}
\mathbf{J} &= \frac{\omega_n}{2\pi} \frac{e}{4\pi r_n^2} N[\delta(r-r_n)] \text{Re}\{Y_\ell^m(\theta, \phi)\} [\mathbf{u}(t) \times \mathbf{r}] \\
&= \frac{\omega_n}{2\pi} \frac{e}{4\pi r_n^2} N[\delta(r-r_n)] (P_\ell^m(\cos\theta) \cos(m\phi + \omega_n t)) [\mathbf{u} \times \mathbf{r}] \\
&= \frac{\omega_n}{2\pi} \frac{e}{4\pi r_n^2} N[\delta(r-r_n)] (P_\ell^m(\cos\theta) \cos(m\phi + \omega_n t)) \sin\theta \hat{\phi}
\end{aligned} \tag{19}$$

where to keep the form of the spherical harmonic as a traveling wave about the z-axis, $\omega_n' = m\omega_n$ and N and N' are normalization constants. The vectors are defined as

$$\hat{\phi} = \frac{\hat{\mathbf{u}} \times \hat{\mathbf{r}}}{|\hat{\mathbf{u}} \times \hat{\mathbf{r}}|} = \frac{\hat{\mathbf{u}} \times \hat{\mathbf{r}}}{\sin\theta}; \quad \hat{\mathbf{u}} = \hat{\mathbf{z}} = \textit{orbital axis} \tag{20}$$

$$\hat{\theta} = \hat{\phi} \times \hat{\mathbf{r}} \tag{21}$$

"^" denotes the unit vectors $\hat{\mathbf{u}} \equiv \frac{\mathbf{u}}{|\mathbf{u}|}$, non-unit vectors are designed in bold, and the current

function is normalized. For the electron source current given by Eq. (19), each comprising a multipole of order (ℓ, m) with a time dependence $e^{i\omega_n t}$, the far-field solutions to Maxwell's equations are given by

$$\mathbf{B} = -\frac{i}{k} a_M(\ell, m) \nabla \times g_\ell(kr) \mathbf{X}_{\ell, m} \tag{22}$$

$$\mathbf{E} = a_M(\ell, m) g_\ell(kr) \mathbf{X}_{\ell, m}$$

and the time-averaged power radiated per solid angle $\frac{dP(\ell, m)}{d\Omega}$ is

$$\frac{dP(\ell, m)}{d\Omega} = \frac{c}{8\pi k^2} |a_M(\ell, m)|^2 |\mathbf{X}_{\ell, m}|^2 \tag{23}$$

where $a_M(\ell, m)$ is

$$a_M(\ell, m) = \frac{-ek^2}{c\sqrt{\ell(\ell+1)}} \frac{\omega_n}{2\pi} N j_\ell(kr_n) \Theta \sin(mks) \tag{24}$$

In the case that k is the lightlike k^0 , then $k = \omega_n / c$, in Eq. (24), and Eqs. (22-23) vanishes for

$$s = vT_n = R = r_n = \lambda_n \tag{25}$$

There is no radiation.

E. Magnetic Field Equations of the Electron

The orbitsphere is a shell of negative charge current comprising correlated charge motion along great circles. For $\mathfrak{l} = 0$, the orbitsphere gives rise to a magnetic moment of 1 Bohr magneton [32]. (The details of the derivation of the magnetic parameters including the electron g factor are given in Ref. [3] and Chp. 1 of Ref. [1].)

$$\mu_B = \frac{e\hbar}{2m_e} = 9.274 \times 10^{-24} \text{ JT}^{-1} \tag{26}$$

The magnetic field of the electron shown in Figure 5 is given by

$$\mathbf{H} = \frac{e\hbar}{m_e r_n^3} (\mathbf{i}_r \cos \theta - \mathbf{i}_\theta \sin \theta) \quad \text{for } r < r_n \quad (27)$$

$$\mathbf{H} = \frac{e\hbar}{2m_e r^3} (\mathbf{i}_r 2 \cos \theta + \mathbf{i}_\theta \sin \theta) \quad \text{for } r > r_n \quad (28)$$

The energy stored in the magnetic field of the electron is

$$E_{mag} = \frac{1}{2} \mu_o \int_0^{2\pi} \int_0^\pi \int_0^\infty H^2 r^2 \sin \theta dr d\theta d\Phi \quad (29)$$

$$E_{mag \text{ total}} = \frac{\pi \mu_o e^2 \hbar^2}{m_e^2 r_1^3} \quad (30)$$

F. Stern-Gerlach Experiment

The Stern-Gerlach experiment implies a magnetic moment of one Bohr magneton and an associated angular momentum quantum number of 1/2. Historically, this quantum number is called the spin quantum number, s ($s = \frac{1}{2}$; $m_s = \pm \frac{1}{2}$). The superposition of the vector projection of the orbitsphere angular momentum on the z-axis is $\frac{\hbar}{2}$ with an orthogonal component of $\frac{\hbar}{4}$. Excitation of a resonant Larmor precession gives rise to \hbar on an axis \mathbf{S} that precesses about the z-axis called the spin axis at the Larmor frequency at an angle of $\theta = \frac{\pi}{3}$ to give a perpendicular projection of

$$\mathbf{S}_\perp = \hbar \sin \frac{\pi}{3} = \pm \sqrt{\frac{3}{4}} \hbar \mathbf{i}_{Y_R} \quad (31)$$

and a projection onto the axis of the applied magnetic field of

$$\mathbf{S}_\parallel = \hbar \cos \frac{\pi}{3} = \pm \frac{\hbar}{2} \mathbf{i}_z \quad (32)$$

The superposition of the $\frac{\hbar}{2}$, z-axis component of the orbitsphere angular momentum and the $\frac{\hbar}{2}$, z-axis component of \mathbf{S} gives \hbar corresponding to the observed electron magnetic moment of a Bohr magneton, μ_B .

G. Electron g Factor

Conservation of angular momentum of the orbitsphere permits a discrete change of its “kinetic angular momentum” ($\mathbf{r} \times m\mathbf{v}$) by the applied magnetic field of $\frac{\hbar}{2}$, and concomitantly the “potential angular momentum” ($\mathbf{r} \times e\mathbf{A}$) must change by $-\frac{\hbar}{2}$.

$$\Delta \mathbf{L} = \frac{\hbar}{2} - \mathbf{r} \times e\mathbf{A} \quad (33)$$

$$= \left[\frac{\hbar}{2} - \frac{e\phi}{2\pi} \right] \hat{z} \quad (34)$$

In order that the change of angular momentum, $\Delta\mathbf{L}$, equals zero, ϕ must be $\Phi_0 = \frac{h}{2e}$, the magnetic flux quantum. The magnetic moment of the electron is parallel or antiparallel to the applied field only. During the spin-flip transition, power must be conserved. Power flow is governed by the Poynting power theorem,

$$\nabla \cdot (\mathbf{E} \times \mathbf{H}) = -\frac{\partial}{\partial t} \left[\frac{1}{2} \mu_o \mathbf{H} \cdot \mathbf{H} \right] - \frac{\partial}{\partial t} \left[\frac{1}{2} \epsilon_o \mathbf{E} \cdot \mathbf{E} \right] - \mathbf{J} \cdot \mathbf{E} \quad (35)$$

Eq. (36) gives the total energy of the flip transition which is the sum of the energy of reorientation of the magnetic moment (1st term), the magnetic energy (2nd term), the electric energy (3rd term), and the dissipated energy of a fluxon treading the orbitsphere (4th term), respectively,

$$\Delta E_{mag}^{spin} = 2 \left(1 + \frac{\alpha}{2\pi} + \frac{2}{3} \alpha^2 \left(\frac{\alpha}{2\pi} \right) - \frac{4}{3} \left(\frac{\alpha}{2\pi} \right)^2 \right) \mu_B B \quad (36)$$

$$\Delta E_{mag}^{spin} = g \mu_B B \quad (37)$$

where the stored magnetic energy corresponding to the $\frac{\partial}{\partial t} \left[\frac{1}{2} \mu_o \mathbf{H} \cdot \mathbf{H} \right]$ term increases, the stored electric energy corresponding to the $\frac{\partial}{\partial t} \left[\frac{1}{2} \epsilon_o \mathbf{E} \cdot \mathbf{E} \right]$ term increases, and the $\mathbf{J} \cdot \mathbf{E}$ term is dissipative. The spin-flip transition can be considered as involving a magnetic moment of g times that of a Bohr magneton. The g factor is redesignated the fluxon g factor as opposed to the anomalous g factor. Using $\alpha^{-1} = 137.03603(82)$, the calculated value of $\frac{g}{2}$ is 1.001 159 652 137. The experimental value [33] of $\frac{g}{2}$ is 1.001 159 652 188(4).

H. Spin and Orbital Parameters

The total function that describes the spinning motion of each electron orbitsphere is composed of two functions. One function, the spin function, is spatially uniform over the orbitsphere, spins with a quantized angular velocity, and gives rise to spin angular momentum. The other function, the modulation function, can be spatially uniform—in which case there is no orbital angular momentum and the magnetic moment of the electron orbitsphere is one Bohr magneton—or not spatially uniform—in which case there is orbital angular momentum. The modulation function also rotates with a quantized angular velocity.

The spin function of the electron corresponds to the nonradiative $n = 1$, $\ell = 0$ state of atomic hydrogen which is well known as an s state or orbital. (See Figure 1 for the charge

function and Figure 2 for the current function.) In cases of orbitals of heavier elements and excited states of one electron atoms and atoms or ions of heavier elements with the ℓ quantum number not equal to zero and which are not constant as given by Eq. (14), the constant spin function is modulated by a time and spherical harmonic function as given by Eq. (15) and shown in Figure 3. The modulation or traveling charge density wave corresponds to an orbital angular momentum in addition to a spin angular momentum. These states are typically referred to as p, d, f, etc. orbitals. Application of Haus's [26] condition also predicts nonradiation for a constant spin function modulated by a time and spherically harmonic orbital function. There is acceleration without radiation as also shown in Sec. IIDc. (Also see Abbott and Griffiths, Goedecke, and Daboul and Jensen [29-31]). However, in the case that such a state arises as an excited state by photon absorption, it is radiative due to a radial dipole term in its current density function since it possesses spacetime Fourier Transform components synchronous with waves traveling at the speed of light [26]. (See Instability of Excited States section of Ref. [1].)

a. Moment of Inertia and Spin and Rotational Energies

The moments of inertia and the rotational energies as a function of the ℓ quantum number for the solutions of the time-dependent electron charge density functions (Eqs. (14-15)) given in Sec. IIC are solved using the rigid rotor equation [28]. The details of the derivations of the results as well as the demonstration that Eqs. (14-15) with the results given *infra.* are solutions of the wave equation are given in Chp 1, Rotational Parameters of the Electron (Angular Momentum, Rotational Energy, Moment of Inertia) section of Ref. [1].

$$\ell = 0$$

$$I_z = I_{spin} = \frac{m_e r_n^2}{2} \quad (38)$$

$$L_z = I\omega_z = \pm \frac{\hbar}{2} \quad (39)$$

$$E_{rotational} = E_{rotational, spin} = \frac{1}{2} \left[I_{spin} \left(\frac{\hbar}{m_e r_n^2} \right)^2 \right] = \frac{1}{2} \left[\frac{m_e r_n^2}{2} \left(\frac{\hbar}{m_e r_n^2} \right)^2 \right] = \frac{1}{4} \left[\frac{\hbar^2}{2I_{spin}} \right] \quad (40)$$

$$T = \frac{\hbar^2}{2m_e r_n^2} \quad (41)$$

$$\ell \neq 0$$

$$I_{orbital} = m_e r_n^2 \left[\frac{\ell(\ell+1)}{\ell^2 + 2\ell + 1} \right]^{\frac{1}{2}} = m_e r_n^2 \sqrt{\frac{\ell}{\ell+1}} \quad (42)$$

$$\mathbf{L} = I \boldsymbol{\omega}_z = I_{orbital} \boldsymbol{\omega}_z = m_e r_n^2 \left[\frac{\ell(\ell+1)}{\ell^2 + 2\ell + 1} \right]^{\frac{1}{2}} \boldsymbol{\omega}_z = m_e r_n^2 \frac{\hbar}{m_e r_n^2} \sqrt{\frac{\ell}{\ell+1}} = \hbar \sqrt{\frac{\ell}{\ell+1}} \quad (43)$$

$$L_{z\ total} = L_{z\ spin} + L_{z\ orbital} \quad (44)$$

$$E_{rotational\ orbital} = \frac{\hbar^2 \left[\frac{\ell(\ell+1)}{\ell^2 + 2\ell + 1} \right]}{2I} = \frac{\hbar^2 \left[\frac{\ell}{\ell+1} \right]}{2I} = \frac{\hbar^2 \left[\frac{\ell}{\ell+1} \right]}{2m_e r_n^2} \quad (45)$$

$$\langle L_{z\ orbital} \rangle = 0 \quad (46)$$

$$\langle E_{rotational\ orbital} \rangle = 0 \quad (47)$$

The orbital rotational energy arises from a spin function (spin angular momentum) modulated by a spherical harmonic angular function (orbital angular momentum). The time-averaged mechanical angular momentum and rotational energy associated with the wave-equation solution comprising a traveling charge-density wave on the orbisphere is zero as given in Eqs. (46) and (47), respectively. Thus, the principal levels are degenerate except when a magnetic field is applied. In the case of an excited state, the angular momentum of \hbar is carried by the fields of the trapped photon. The amplitudes that couple to external magnetic and electromagnetic fields are given by Eq. (43) and (45), respectively. The rotational energy due to spin is given by Eq. (40), and the total kinetic energy is given by Eq. (41).

I. Force Balance Equation

The radius of the nonradiative ($n=1$) state is solved using the electromagnetic force equations of Maxwell relating the charge and mass density functions wherein the angular momentum of the electron is given by \hbar [1]. The reduced mass arises naturally from an electrodynamic interaction between the electron and the proton of mass m_p .

$$\frac{m_e v_1^2}{4\pi r_1^2} = \frac{e}{4\pi \epsilon_1^2} \frac{Ze}{4\pi \epsilon_o r_1^2} - \frac{1}{4\pi \epsilon_1^2} \frac{\hbar^2}{m_p r_n^3} \quad (48)$$

$$r_1 = \frac{a_H}{Z} \quad (49)$$

where a_H is the radius of the hydrogen atom.

J. Energy Calculations

From Maxwell's equations, the potential energy V , kinetic energy T , electric energy or binding energy E_{ele} are

$$V = \frac{-Ze^2}{4\pi \epsilon_o r_1} = \frac{-Z^2 e^2}{4\pi \epsilon_o a_H} = -Z^2 \times 4.3675 \times 10^{-18} \text{ J} = -Z^2 \times 27.2 \text{ eV} \quad (50)$$

$$T = \frac{Z^2 e^2}{8\pi\epsilon_0 a_H} = Z^2 \times 13.59 \text{ eV} \quad (51)$$

$$T = E_{ele} = -\frac{1}{2} \epsilon_0 \int_{\infty}^{r_1} \mathbf{E}^2 dv \quad \text{where } \mathbf{E} = -\frac{Ze}{4\pi\epsilon_0 r^2} \quad (52)$$

$$E_{ele} = -\frac{Ze^2}{8\pi\epsilon_0 r_1} = -\frac{Z^2 e^2}{8\pi\epsilon_0 a_H} = -Z^2 \times 2.1786 \times 10^{-18} \text{ J} = -Z^2 \times 13.598 \text{ eV} \quad (53)$$

The calculated Rydberg constant is $10,967,758 \text{ m}^{-1}$; the experimental Rydberg constant is $10,967,758 \text{ m}^{-1}$. For increasing Z , the velocity becomes a significant fraction of the speed of light; thus, special relativistic corrections were included in the calculation of the ionization energies of one-electron atoms that are given in Table 1.

K. Two Electron Atoms

Two electron atoms may be solved from a central force balance equation with the nonradiation condition [1]. The centrifugal force, $\mathbf{F}_{centrifugal}$, of each electron is given by

$$\mathbf{F}_{centrifugal} = \frac{m_e \mathbf{v}_n^2}{r_n} \quad (54)$$

where r_n is the radius of electron n which has velocity \mathbf{v}_n . In order to be nonradiative, the velocity for every point on the orbitsphere is given by Eq. (6). Now, consider electron 1 initially at $r = r_1 = \frac{a_0}{Z}$ (the radius of the one-electron atom of charge Z given in the Sec. II I where $a_0 = \frac{4\pi\epsilon_0 \hbar^2}{e^2 m_e}$ and the spin-nuclear interaction corresponding to the electron reduced mass is not

used here since the electrons have no field at the nucleus upon pairing) and electron 2 initially at $r_n = \infty$. Each electron can be treated as $-e$ charge at the nucleus with $\mathbf{E} = \frac{-e}{4\pi\epsilon_0 r^2}$ for $r > r_n$ and $\mathbf{E} = 0$ for $r < r_n$ where r_n is the radius of the electron orbitsphere. The centripetal force is the electric force, \mathbf{F}_{ele} , between the electron and the nucleus. Thus, the electric force between electron 2 and the nucleus is

$$\mathbf{F}_{el(electron\ 2)} = \frac{(Z-1)e^2}{4\pi\epsilon_0 r_2^2} \quad (55)$$

where ϵ_0 is the permittivity of free-space. The second centripetal force, \mathbf{F}_{mag} , on the electron 2 (initially at infinity) from electron 1 (at r_1) is the magnetic force. Due to the relative motion of the charge-density elements of each electron, a radiation reaction force arises between the two electrons. This force given in Sections 6.6, 12.10, and 17.3 of Jackson [38] achieves the condition that the sum of the mechanical momentum and electromagnetic momentum is conserved. The magnetic central force is derived from the Lorentzian force which is relativistically corrected. The magnetic field of electron 2 at the radius of electron 1 follows

from Eq. (1.74b) of Ref. [1] after McQuarrie [32]:

$$\mathbf{B} = \frac{\mu_0 e \hbar}{2 m_e r_2^3} \quad (56)$$

where μ_0 is the permeability of free-space ($4\pi \times 10^{-7} \text{ N / A}^2$). The motion at each point of electron 1 in the presence of the magnetic field of electron 2 gives rise to a central force which acts at each point of electron 2. The Lorentzian force density at each point moving at velocity \mathbf{v} given by Eq. (6) is

$$\mathbf{F}_{mag} = \frac{e}{4\pi r_2^2} \mathbf{v} \times \mathbf{B} \quad (57)$$

Substitution of Eq. (6) for \mathbf{v} and Eq. (56) for \mathbf{B} gives

$$\mathbf{F}_{mag} = \frac{1}{4\pi r_2^2} \left[\frac{e^2 \mu_0}{2 m_e r_1} \right] \frac{\hbar^2}{m_e r_2^3} \quad (58)$$

The term in brackets can be expressed in terms of the fine structure constant α . The radius of the electron orbitsphere in the $v = c$ frame is λ_c , where $v = c$ corresponds to the magnetic field front propagation velocity which is the same in all inertial frames, independent of the electron velocity as shown by the velocity addition formula of special relativity [39]. From Eq. (7) and Eqs. (1.144-1.148) of Ref. [1]

$$\frac{e^2 \mu_0}{2 m_e r_1} = 2\pi\alpha \frac{v}{c} \quad (59)$$

where $v = c$. Based on the relativistic invariance of the electron's magnetic moment of a Bohr magneton $\mu_B = \frac{e\hbar}{2m_e}$ as well as its invariant angular momentum of \hbar , it can be shown that the

relativistic correction to Eq. (58) is $\frac{1}{Z}$ times the reciprocal of Eq. (59). In addition, as given in the Spin Angular Momentum of the Orbitsphere with $\ell = 0$ section of Ref [1], the application of a z directed magnetic field of electron 2 given by Eq. (1.120) of Ref. [1] to the inner orbitsphere gives rise to a projection of the angular momentum of electron 1 onto an axis which precesses about the z-axis of $\sqrt{\frac{3}{4}}\hbar$. The projection of the force between electron 2 and electron 1 is equivalent to that of the angular momentum onto the axis which precesses about the z-axis. Thus, Eq. (58) becomes

$$\mathbf{F}_{mag} = \frac{1}{4\pi r_2^2} \frac{1}{Z} \frac{\hbar^2}{m_e r_2^3} \sqrt{s(s+1)} \quad (60)$$

Using Eq. (6), the outward centrifugal force on electron 2 is balanced by the electric force and the magnetic force (on electron 2),

$$\frac{m_e}{4\pi r_2^2} \frac{v_2^2}{r_2} = \frac{m_e}{4\pi r_2^2} \frac{\hbar^2}{m_e r_2^3} = \frac{e}{4\pi r_2^2} \frac{(Z-1)e}{4\pi \epsilon_0 r_2^2} + \frac{1}{4\pi r_2^2} \frac{\hbar^2}{Z m_e r_2^3} \sqrt{s(s+1)} \quad (61)$$

which gives the radius of both electrons as

$$r_2 = r_1 = a_0 \left(\frac{1}{Z-1} - \frac{\sqrt{s(s+1)}}{Z(Z-1)} \right); \quad s = \frac{1}{2} \quad (62)$$

(Since the density factor always cancels, it will not be used in subsequent force balance equations).

a. Ionization Energies Calculated using the Poynting Power Theorem

During ionization, power must be conserved. Power flow is governed by the Poynting power theorem given by Eq. (35). Energy is superposable; thus, the calculation of the ionization energy is determined as a sum of the electric and magnetic contributions. Energy must be supplied to overcome the electric force of the nucleus, and this energy contribution is the negative of the electric work given by Eq. (64). Additionally, the electrons are initially spin paired at $r_1 = r_2 = 0.566987a_0$ producing no magnetic fields; whereas, following ionization, the electrons possess magnetic fields and corresponding energies. For helium, the contribution to the ionization energy is given as the energy stored in the magnetic fields of the two electrons at the initial radius where they become spin unpaired. Part of this energy and the corresponding relativistic term correspond to the precession of the outer electron about the z-axis due to the spin angular momentum of the inner electron. These terms are the same as those of the corresponding terms of the hyperfine structure interval of muonium as given in the Muonium Hyperfine Structure Interval section of Ref [1]. Thus, for helium, which has no electric field beyond r_1 the ionization energy is given by the general formula:

$$\text{Ionization Energy}(He) = -E(\text{electric}) + E(\text{magnetic}) \left(1 - \frac{1}{2} \left(\left(\frac{2}{3} \cos \frac{\pi}{3} \right)^2 + \alpha \right) \right) \quad (63)$$

where,

$$E(\text{electric}) = -\frac{(Z-1)e^2}{8\pi\epsilon_0 r_1} \quad (64)$$

$$E(\text{magnetic}) = \frac{2\pi\mu_0 e^2 \hbar^2}{m_e^2 r_1^3} = \frac{8\pi\mu_0 \mu_B^2}{r_1^3} \quad (65)$$

Eq. (65) is derived for each of the two electrons as Eq. (1.129) of the Magnetic Parameters of the Electron (Bohr Magnetron) section of Ref. [1] with the radius given by Eq. (62).

For $3 \leq Z$, a quantized electric field exists for $r > r_1$ that gives rise to a dissipative term, $\mathbf{J} \bullet \mathbf{E}$, of the Poynting Power Vector given by Eq. (35). Thus, the ionization energies are given by

$$\text{Ionization Energy} = -\text{Electric Energy} - \frac{1}{Z} \text{Magnetic Energy} \quad (66)$$

With the substitution of the radius given by Eq. (62) into Eq. (6), the velocity v is given by

$$v = \frac{\hbar c}{\sqrt{\left(\frac{4\pi\epsilon_0\hbar^2}{e^2} c \left(\frac{1}{Z-1} - \frac{\sqrt{\frac{3}{4}}}{Z(Z-1)} \right) \right)^2 + \hbar^2}} = \frac{\alpha c(Z-1)}{\sqrt{\left(1 - \frac{\sqrt{\frac{3}{4}}}{Z} \right)^2 + \alpha^2(Z-1)^2}} \quad (67)$$

with $Z > 1$. For increasing Z , the velocity becomes a significant fraction of the speed of light; thus, special relativistic corrections as given in the Special Relativistic Correction to the Ionization Energies section of Ref. [1] and Sec. IIDa were included in the calculation of the ionization energies of two-electron atoms given in Table 2. The calculated ionization energy for helium is 24.58750 eV and the experimental ionization energy is 24.58741 eV. The agreement in the values is within the limit set by experimental error [19].

The solution of the helium atom is further proven to be correct since it is used to solve up through twenty-electron atoms in the Three, Four, Five, Six, Seven, Eight, Nine, Ten, Eleven, Twelve, Thirteen, Fifteen, Sixteen, Seventeen, Eighteen, Nineteen, and Twenty-Electron Atoms section of Ref. [1]. The predictions from general solutions for one through twenty-electron atoms are in remarkable agreement with the experimental values known for 400 atoms and ions.

III. Classical Scattering

A. Far Field Pattern

In Fourier optics, the classical far field pattern involving Fraunhofer diffraction as the dominant mode of scattering is given by the Fourier transform of the aperture function. As given previously in the Classical Photon and Electron Scattering section of Ref. [1], the aperture function is given by the convolution of the array function with the elemental pattern. Huygens' principle is that a point source will give rise to a spherical wave emanating equally in all directions, and the waves from multiple such point sources superimpose. An arbitrary wave shape may be considered as a collection of point sources whose strength is given by the amplitude of the wave at that point. The field, at any point in space, is simply a sum of spherical waves. The asymptotic total amplitude of N such point sources is expressible as an outgoing spherical wave corresponding to a Green function source:

$$\Psi_{total} = \frac{e^{ikR}}{R} \sum_{l=1}^N e^{is_r} f_l(\theta, \phi) \quad (68)$$

Applying Huygens' principle to a disturbance across a plane aperture gives the amplitude of the far field as the Fourier transform of the aperture distribution, i.e., apart from constant factors,

$$\psi(x, y) = \iint A(\xi, \eta) \exp\left[\frac{-ik}{f}(\xi x + \eta y)\right] d\xi d\eta \quad (69)$$

Here $A(\xi, \eta)$ describes the amplitude and phase distribution across the aperture and $\psi(x, y)$ describes the far field [40] where f is the focal length. The classical theory then gives the intensity as the square magnitude of the scattered amplitude.

B. Two-Slit Interference (Wave-Particle Duality)

The classical solution of single photons is given in the Equation of the Photon section of Ref. [1]. Photons superimpose such that in the far field the emitted wave is a spherical wave where the total electric field is given by Eq. (4.23) of Ref [1]:

$$\mathbf{E}_{total} = E_o \frac{e^{-ikr}}{r} \quad (70)$$

which is shown by Bonham to be required in order to insure continuity of power flow for wavelets from a single source [41]. The Green Function, (Eq. (6.62) of Jackson [42]) is given as the solution of the wave equation (Eq. (6.58) of Jackson [42]). Thus, the superposition of photons gives the classical result. As r goes to infinity, the spherical wave given by Eq. (70) becomes a plane wave. The double slit interference pattern is derived in Eqs. (71-79). From the equation of a photon (Eqs. (4.4-4.7) of Ref. [1]), the wave-particle duality arises naturally. The energy is always given by Planck's equation as shown in Ref. [1]; yet, an interference pattern is observed when photons add over time or space.

Similarly, rather than a point, the electron is an extended particle which may impinge on a double slit one electron at a time. As shown in the Electron in Free Space section of Ref. [1], the ionized electron is a plane-lamina disc of charge (mass)-density given by Eqs. (3.7-3.8) and current (momentum)-density given by Eqs. (3.11) and (3.13) of Ref. [1] with a radius ρ_o such that $2\pi\rho_o = \lambda_o$ wherein λ_o is the de Broglie wavelength. In the case that the electron de Broglie wavelength (Eq. (5)) and therefore the size of the electron is comparable to the slit size and separation, the resulting intensity pattern of electrons striking a detector beyond the slits is equivalent to a wave interference pattern. This result arises even though the electrons are not physically interacting with each other. Nothing is actually interfering. As in the case of the photon, the wave-particle duality nature of the electron arises classically.

The simplest of interference experiments, Young's double-slit experiment in one dimension is given in the Classical Photon and Electron Scattering section of Ref. [1]. We use the array theorem which states that the diffraction pattern of an array of similar apertures is given by the product of the Fourier transform of the elemental pattern, $\tilde{\psi}(x)$, and the Fourier transform of the pattern that would be obtained by a similar array of point sources, $\tilde{A}(x)$. The individual aperture will be described by

$$\Psi(\xi) = (C \quad |\xi| < a; \quad 0 \quad |\xi| > a) = rec(\xi|a) \quad (71)$$

Here C is a constant representing the amplitude transmission of the apertures. This is essentially

a one-dimensional problem and the diffraction integral may be written as

$$\tilde{\Psi}(\mathbf{x}) = \int \psi(\xi) \exp\left(\frac{-ik\xi \cdot \mathbf{x}}{f}\right) d\xi = C \int_{-a}^a \exp\left(\frac{-ik\xi \cdot \mathbf{x}}{f}\right) d\xi \quad (72)$$

The integral in Eq. (72) is readily evaluated to give

$$\tilde{\Psi}(\mathbf{x}) = \frac{-Cf}{ikx} \left[\exp\left(\frac{-ikax}{f}\right) - \exp\left(\frac{+ikax}{f}\right) \right] = 2aC \frac{\sin\left(\frac{kax}{f}\right)}{\left(\frac{kax}{f}\right)} \quad (73)$$

The notation $\text{sinc}\theta = \frac{\sin\theta}{\theta}$ is frequently used and in terms of this function $\tilde{\Psi}(\mathbf{x})$ may be written as

$$\tilde{\Psi}(\mathbf{x}) = 2aC \text{sinc}\left(\frac{kax}{f}\right) \quad (74)$$

Thus, the result is that the elemental distribution in the Fraunhofer plane is Eq. (74). The array in this case is simply two delta functions; thus,

$$A(\xi) = \delta(\xi - b) + \delta(\xi + b) \quad (75)$$

The array pattern is, therefore,

$$\tilde{A}(\mathbf{x}) = \int [\delta(\xi - b) + \delta(\xi + b)] \exp\left(\frac{-2\pi i \xi \cdot \mathbf{x}}{\lambda f}\right) d\xi \quad (76)$$

Eq. (76) is readily evaluated by using the combining property of the delta function, thus,

$$\tilde{A}(\mathbf{x}) = \exp\left(\frac{2\pi i b x}{\lambda f}\right) + \exp\left(\frac{-2\pi i b x}{\lambda f}\right) = 2 \cos\left(\frac{2\pi b x}{\lambda f}\right) \quad (77)$$

Finally, the diffraction pattern of the array of two slits is

$$\tilde{\Psi}(\mathbf{x}) = 4aC \text{sinc}\left(\frac{2\pi a x}{\lambda f}\right) \cos\left(\frac{2\pi b x}{\lambda f}\right) \quad (78)$$

The intensity is

$$I(\mathbf{x}) = 16a^2 C^2 \text{sinc}^2\left(\frac{2\pi a x}{\lambda f}\right) \cos^2\left(\frac{2\pi b x}{\lambda f}\right) \quad (79)$$

From Eq. (79), it is clear that the resulting pattern has the appearance of cosine-squared fringes of period $\lambda f / b$ with an envelope $\text{sinc}^2(2\pi a x / \lambda f)$. The distribution pattern observed with diffracting electrons is equivalent to that for diffracting light. Note that Eq. (72) represents a plane wave. In the case of the Davison-Germer experiment, the intensity is given by the array theorem as the product of the Fourier transforms of the elemental pattern corresponding to a plane wave of wavelength $\lambda = h / p$ and the array pattern of the nickel crystal.

C. Electron Scattering from Helium

Consider the case of monoenergetic electrons elastically scattering from helium atoms. The helium atom comprises nucleus of charge $+2e$ which is at the center of an infinitely thin

spherical shell at the radius of (Eq. (62))

$$r_1 = r_2 = 0.566987a_0 \quad (80)$$

comprising two spin-paired bound electrons of $-2e$. Thus, the helium atom is neutral charged with no magnetic field, and the electric field of the atom is zero for $r > 0.566987a_0$. The Rutherford scattering equation for isolated charged particles does *not* apply. According to Huygens' principle, the outgoing wave is given by the integral over each spherical wave source arising from the scattering of an incident plane wave from each point of the electron function where the wavelength of the incident plane wave is given by the de Broglie equation $\lambda = h/p$ and the electrons are continuous surfaces. As shown in the Classical Wave Theory of Electron Scattering section of Ref. [1], the integral over ρ and ϕ of the corresponding single point element aperture distribution function gives the aperture array distribution function, $A(z)$, and $F(s)$, the Fourier transform of $A(z)$, gives the far-field amplitude of the scattered incident electron plane wave. The general Fourier transform integral is given in reference [43]. For an aperture distribution with circular symmetry, the integral of $a(\rho, \phi, z)$ over ρ and ϕ and $F(s)$, the Fourier transform of $A(z)$, is given by [43]:

$$\begin{aligned} F(s) &= 2\pi \int_0^{\infty} \int_{-\infty}^{\infty} a(\rho, z) J_0(s\rho) e^{-iws} \rho d\rho dz \\ &= \int_0^{\infty} A(z) e^{-iws} dz \end{aligned} \quad (81)$$

The aperture distribution function, $a(\rho, \phi, z)$, for the scattering of an incident plane wave by the He atom is given by the convolution of the plane wave function with the two electron orbitsphere Dirac delta function of *radius* = $0.567a_0$ and charge/mass density of $\frac{2}{4\pi(0.567a_0)^2}$.

For radial units in terms of a_0 :

$$a(\rho, \phi, z) = \pi(z) \otimes \frac{2}{4\pi(0.567a_0)^2} [\delta(r - 0.567a_0)] \quad (82)$$

where $a(\rho, \phi, z)$ is given in cylindrical coordinates, $\pi(z)$, the xy-plane wave is given in Cartesian coordinates with the propagation direction along the z-axis, and the He atom orbitsphere function, $\frac{2}{4\pi(0.567a_0)^2} [\delta(r - 0.567a_0)]$, is given in spherical coordinates. The

convolution gives

$$a(\rho, \phi, z) = \frac{2}{4\pi(0.567a_0)^2} \sqrt{(0.567a_0)^2 - z^2} \delta(r - \sqrt{(0.567a_0)^2 - z^2}) \quad (83)$$

For circular symmetry [43],

$$F(s) = \frac{2}{4\pi(0.567a_0)^2} 2\pi \int_0^{\infty} \int_{-\infty}^{\infty} \sqrt{(0.567a_0)^2 - z^2} \delta(\rho - \sqrt{(0.567a_0)^2 - z^2}) J_0(s\rho) e^{-iws} \rho d\rho dz \quad (84)$$

Eq. (84) may be expressed as

$$F(s) = \frac{4\pi}{4\pi(0.567a_0)^2} \int_{-z_0}^{z_0} (z_0^2 - z^2) J_0(s\sqrt{z_0^2 - z^2}) e^{-iwz} dz ; z_0 = 0.567a_0 \quad (85)$$

Substitution of $\frac{z}{z_0} = -\cos\theta$ into Eq. (85) gives

$$F(s) = \frac{4\pi z_0^2}{4\pi z_0^2} \int_0^\pi \sin^3\theta J_0(sz_0 \sin\theta) e^{iz_0 w \cos\theta} d\theta \quad (86)$$

Substitution of the recurrence relationship,

$$J_0(x) = \frac{2J_1(x)}{x} - J_2(x) ; x = sz_0 \sin\theta \quad (87)$$

into Eq. (86), and, using the general integral of Apelblat [44]:

$$\int_0^\pi (\sin\theta)^{\nu+1} J_\nu(b \sin\theta) e^{ia \cos\theta} d\theta = \left[\frac{2\pi}{a^2 + b^2} \right]^{\frac{1}{2}} \left[\frac{b}{a^2 + b^2} \right]^\nu J_{\nu+1/2} \left[(a^2 + b^2)^{\frac{1}{2}} \right] \quad (88)$$

with $a = z_0 w$ and $b = z_0 s$ gives:

$$F(s) = \left[\frac{2\pi}{(z_0 w)^2 + (z_0 s)^2} \right]^{\frac{1}{2}} \left\{ 2 \left[\frac{z_0 s}{(z_0 w)^2 + (z_0 s)^2} \right] J_{3/2} \left[((z_0 w)^2 + (z_0 s)^2)^{1/2} \right] - \left[\frac{z_0 s}{(z_0 w)^2 + (z_0 s)^2} \right]^2 J_{5/2} \left[((z_0 w)^2 + (z_0 s)^2)^{1/2} \right] \right\} \quad (89)$$

The electron elastic scattering intensity is given by a constant times the square of the amplitude given by Eq. (89):

$$I_1^{ed} = I_e \left\{ \left[\frac{2\pi}{(z_0 w)^2 + (z_0 s)^2} \right]^{\frac{1}{2}} \left\{ 2 \left[\frac{z_0 s}{(z_0 w)^2 + (z_0 s)^2} \right] J_{3/2} \left[((z_0 w)^2 + (z_0 s)^2)^{1/2} \right] - \left[\frac{z_0 s}{(z_0 w)^2 + (z_0 s)^2} \right]^2 J_{5/2} \left[((z_0 w)^2 + (z_0 s)^2)^{1/2} \right] \right\} \right\}^2 \quad (90)$$

$$s = \frac{4\pi}{\lambda} \sin \frac{\theta}{2}; w = 0 \text{ (units of } \text{\AA}^{-1}) \quad (91)$$

The experimental results of Bromberg [45], the extrapolated experimental data of Hughes [45], the small angle data of Geiger [46], and the semiexperimental results of Lassetre [45] for the elastic differential cross section for the elastic scattering of electrons by helium atoms are shown graphically in Figure 6. The elastic differential cross section as a function of angle numerically calculated by Khare [45] using the first Born approximation and first-order

exchange approximation also appear in Figure 6. These results which are based on a quantum mechanical model are compared with experimentation [45, 46]. The closed-form function (Eqs. (90) and (91)) for the elastic differential cross section for the elastic scattering of electrons by helium atoms is shown graphically in Figure 7. The scattering amplitude function, $F(s)$ (Eq. (89)), is shown as an insert. The Maxwellian, exact orbitsphere model provides a continuous representation of all states of the electron including the ionized state as a plane wave having the de Broglie wavelength. Using the exact, unique solution of the helium atom, in a closed-form solution, the Maxwellian model predicts the experimental results of the electron scattering from helium for all angles. Next, the same CQM solution for the helium atom is used to calculate the helium excited states.

IV. Excited States of Helium

Each orbitsphere is a spherical shell of negative charge (total charge $= -e$) of zero thickness at a distance r_n from the nucleus (charge $= +Ze$). It is well known that the field of a spherical shell of charge is zero inside the shell and that of a point charge at the origin outside the shell [47]. The field of each electron can be treated as that corresponding to a $-e$ charge at the origin with $\mathbf{E} = \frac{-e}{4\pi\epsilon_0 r^2}$ for $r > r_n$ and $\mathbf{E} = 0$ for $r < r_n$ where r_n is the radius of the electron orbitsphere. Thus, as shown in the Two-Electron Atom section of Ref. [1] and Sec. IIK, the central electric fields due to the helium nucleus are $\mathbf{E} = \frac{2e}{4\pi\epsilon_0 r^2}$ and $\mathbf{E} = \frac{e}{4\pi\epsilon_0 r^2}$ for $r < r_1$ and $r_1 < r < r_2$, respectively. In the ground state of the helium atom, both electrons are at $r_1 = r_2 = 0.566987a_0$. When a photon is absorbed, one of the initially indistinguishable electrons called electron 1 moves to a smaller radius, and the other called electron 2 moves to a greater radius. In the limiting case of the absorption of an ionizing photon, electron 1 moves to the radius of the helium ion, $r_1 = 0.5a_0$, and electron 2 moves to a continuum radius, $r_2 = \infty$. When a photon is absorbed by the ground state helium atom it generates an effective charge, Z_{P-eff} , within the second orbitsphere such that the electrons move in opposite radial directions while conserving energy and angular momentum. We can determine Z_{P-eff} of the "trapped photon" electric field by requiring that the resonance condition is met for photons of discrete energy, frequency, and wavelength for electron excitation in an electromagnetic potential energy well.

It is well known that resonator cavities can trap electromagnetic radiation of discrete resonant frequencies. The orbitsphere is a resonator cavity which traps single photons of discrete frequencies. Thus, photon absorption occurs as an excitation of a resonator mode. The free space photon also comprises a radial Dirac delta function, and the angular momentum of the

photon given by $\mathbf{m} = \int \frac{1}{8\pi c} \text{Re}[\mathbf{r} \times (\mathbf{E} \times \mathbf{B}^*)] dx^4 = \hbar$ in the Photon section of Ref. [1] is conserved [42] for the solutions for the resonant photons and excited state electron functions as shown for one-electron atoms in the Excited States of the One-Electron Atom (Quantization) section of Ref. [1]. The correspondence principle holds. That is the change in angular frequency of the electron is equal to the angular frequency of the resonant photon that excites the resonator cavity mode corresponding to the transition, and the energy is given by Planck's equation. It can be demonstrated that the resonance condition between these frequencies is to be satisfied in order to have a net change of the energy field [48].

In general, for a macroscopic multipole with a single m value, a comparison of Eq. (2.33) and Eq. (2.25) of Ref. [1] shows that the relationship between the angular momentum M_z , energy U , and angular frequency ω is given by Eq. (2.34) of Ref. [1]:

$$\frac{dM_z}{dr} = \frac{m}{\omega} \frac{dU}{dr} \quad (92)$$

independent of r where m is an integer. Furthermore, the ratio of the square of the angular momentum, M^2 , to the square of the energy, U^2 , for a pure (ℓ, m) multipole follows from Eq. (2.25) and Eqs. (2.31-2.33) as given by Eq. (2.35) of Ref. [1]:

$$\frac{M^2}{U^2} = \frac{m^2}{\omega^2} \quad (93)$$

From Jackson [49], the quantum mechanical interpretation is that the radiation from such a multipole of order (ℓ, m) carries off $m\hbar$ units of the z component of angular momentum per photon of energy $\hbar\omega$. However, the photon and the electron can each possess only \hbar of angular momentum which requires that Eqs. (92-93) correspond to a state of the radiation field containing m photons.

As shown in the Excited States of the One-Electron Atom (Quantization) section of Ref. [1] during excitation the spin, orbital, or total angular momentum of the orbitsphere can change by zero or $\pm \hbar$. The selection rules for multipole transitions between quantum states arise from conservation of the photon's multipole moment and angular momentum of \hbar . In an excited state, the time-averaged mechanical angular momentum and rotational energy associated with the traveling charge-density wave on the orbitsphere is zero (Eqs. (46-47)), and the angular momentum of \hbar of the photon that excites the electronic state is carried by the fields of the trapped photon. The amplitudes of the rotational angular momentum and energy that couple to external magnetic and electromagnetic fields are given by Eq. (43) and (45), respectively. Furthermore, the electron charge-density waves are nonradiative due to the angular motion as shown in the Appendix I: Nonradiation Based on the Electromagnetic Fields and the Poynting Power Vector section of Ref. [1] and Sec. IIDc. But, excited states are radiative due to a radial dipole that arises from the presence of the trapped photon as shown in the Instability of Excited

States section of Ref. [1] corresponding to $m = 1$ in Eqs. (92-93).

Then, as shown in the Excited States of the One-Electron Atom (Quantization) section and the Derivation of the Rotational Parameters of the Electron section of Ref. [1], the total number of multipoles, $N_{\ell,s}$, of an energy level corresponding to a principal quantum number n where each multipole corresponds to an ℓ and m_ℓ quantum number is

$$N_{\ell,s} = \sum_{\ell=0}^{n-1} \sum_{m_\ell=-\ell}^{+\ell} 1 = \sum_{\ell=0}^{n-1} 2\ell + 1 = (\ell + 1)^2 = \ell^2 + 2\ell + 1 = n^2 \quad (94)$$

Any given state may be due to a direct transition or due to the sum of transitions between all intermediate states wherein the multiplicity of possible multipoles increases with higher states. Then, the relationships between the parameters of Eqs. (92) and (93) due to transitions of quantized angular momentum \hbar , energy $\hbar\omega$, and radiative via a radial dipole are given by substitution of $m = 1$ and normalization of the energy U by the total number of degenerate multipoles, n^2 . This requires that the photon's electric field superposes that of the nucleus for $r_1 < r < r_2$ such that the radial electric field has a magnitude proportional to e/n at the electron 2 where $n = 2, 3, 4, \dots$ for excited states such that U is decreased by the factor of $1/n^2$.

Energy is conserved between the electric and magnetic energies of the helium atom as shown by Eq. (7.26) of Ref. [1]. The helium atom and the "trapped photon" corresponding to a transition to a resonant excited state have neutral charge and obey Maxwell's equations. Since charge is relativistically invariant, the energies in the electric and magnetic fields of the electrons of the helium atom must be conserved as photons are emitted or absorbed. The corresponding forces are determined from the requirement that the radial excited-state electric field has a magnitude proportional to e/n at electron 2.

The "trapped photon" is a "standing electromagnetic wave" which actually is a traveling wave that propagates on the surface around the z-axis, and its source current is only at the orbitsphere. The time-function factor, $k(t)$, for the "standing wave" is identical to the time-function factor of the orbitsphere in order to satisfy the boundary (phase) condition at the orbitsphere surface. Thus, the angular frequency of the "trapped photon" has to be identical to the angular frequency of the electron orbitsphere, ω_n , given by Eq. (9). Furthermore, the phase condition requires that the angular functions of the "trapped photon" have to be identical to the spherical harmonic angular functions of the electron orbitsphere. Combining $k(t)$ with the ϕ -function factor of the spherical harmonic gives $e^{i(m\phi - \omega_n t)}$ for both the electron and the "trapped photon" function.

The photon "standing wave" in an excited electronic state is a solution of Laplace's equation in spherical coordinates with source currents given by Eq. (2.11) of Ref. [1] "glued" to the electron and phase-locked to the electron current density wave that travel on the surface with

a radial electric field. As given in the Excited States of the One-Electron Atom (Quantization) section of Ref. [1], the photon field is purely radial since the field is traveling azimuthally at the speed of light even though the spherical harmonic function has a velocity less than light speed given by Eq. (6). The photon field does not change the nature of the electrostatic field of the nucleus or its energy except at the position of the electron. The photon "standing wave" function comprises a radial Dirac delta function that "samples" the Laplace equation solution only at the position infinitesimally inside of the electron current-density function and superimposes with the proton field to give a field of radial magnitude corresponding to a charge of e/n where $n = 2, 3, 4, \dots$.

The electric field of the nucleus for $r_1 < r < r_2$ is

$$\mathbf{E}_{nucleus} = \frac{e}{4\pi\epsilon_0 r^2} \quad (95)$$

From Eq. (2.15) of Ref. [1], the equation of the electric field of the "trapped photon" for $r = r_2$ where r_2 is the radius of electron 2, is

$$\mathbf{E}_{r_{photon} \ n, \ell, m|_{r=r_2}} = \frac{e}{4\pi\epsilon_0 r_2^2} \left[-1 + \frac{1}{n} \left[Y_0^0(\theta, \phi) + \text{Re} \left\{ Y_\ell^m(\theta, \phi) e^{i\omega_n t} \right\} \right] \right] \delta(r - r_n) \\ \omega_n = 0 \text{ for } m = 0 \quad (96)$$

The total central field for $r = r_2$ is given by the sum of the electric field of the nucleus and the electric field of the "trapped photon".

$$\mathbf{E}_{total} = \mathbf{E}_{nucleus} + \mathbf{E}_{photon} \quad (97)$$

Substitution of Eqs. (95) and (96) into Eq. (97) gives for $r_1 < r < r_2$,

$$\mathbf{E}_{r_{total}} = \frac{e}{4\pi\epsilon_0 r_1^2} + \frac{e}{4\pi\epsilon_0 r_2^2} \left[-1 + \frac{1}{n} \left[Y_0^0(\theta, \phi) + \text{Re} \left\{ Y_\ell^m(\theta, \phi) e^{i\omega_n t} \right\} \right] \right] \delta(r - r_n) \\ = \frac{1}{n} \frac{e}{4\pi\epsilon_0 r_2^2} \left[Y_0^0(\theta, \phi) + \text{Re} \left\{ Y_\ell^m(\theta, \phi) e^{i\omega_n t} \right\} \right] \delta(r - r_n) \\ \omega_n = 0 \text{ for } m = 0 \quad (98)$$

For $r = r_2$ and $m = 0$, the total radial electric field is

$$\mathbf{E}_{r_{total}} = \frac{1}{n} \frac{e}{4\pi\epsilon_0 r^2} \quad (99)$$

The result is equivalent to Eq. (2.17) of the Excited States of the One-Electron Atom (Quantization) section of Ref. [1].

In contrast to shortcomings of quantum-mechanical equations, with classical quantum mechanics (CQM), all excited states of the helium atom can be exactly solved in closed form. The radii of electron 2 are determined from the force balance of the electric, magnetic, and centrifugal forces that corresponds to the minimum of energy of the system. The excited-state energies are then given by the electric energies at these radii. All singlet and triplet states with $\ell = 0$ or $\ell \neq 0$ are solved exactly except for small terms corresponding to the magnetostatic

energies in the magnetic fields of excited-state electrons, spin-nuclear interactions, and the very small term due to spin-orbital coupling. In the case of spin-nuclear interactions, a_{He} , which includes the reduced electron mass according to Eqs. (1.221-1.224) of Ref. [1], was used rather than a_0 as a partial correction, and a table of the spin-orbital energies was calculated for $\ell = 1$ to compare to the effect of different ℓ quantum numbers. For over 100 states, the agreement between the predicted and experimental results are remarkable.

A. Singlet Excited States with $\mathbf{l} = \mathbf{0}$ ($1s^2 \rightarrow 1s^1(ns^1)$)

With $\ell = 0$, the electron source current in the excited state is a constant function given by Eq. (14) that spins as a globe about an axis. As given in the Derivation of the Magnetic Field section in Chapter One and by Eq. (12.342) of Ref. [1], the current is a function of $\sin \theta$ which gives rise to a correction of 2/3 to the field given by Eq. (56) and, correspondingly, the magnetic force of two-electron atoms given by Eq. (60). The vector orientations of the electrons and the derivation of the magnetic force is given in Appendix VIII of Ref. [1]. The balance between the centrifugal and electric and magnetic forces is given by the Eq. (61):

$$\frac{m_e v^2}{r_2} = \frac{\hbar^2}{m_e r_2^3} = \frac{1}{n} \frac{e^2}{4\pi\epsilon_0 r_2^2} + \frac{2}{3} \frac{1}{n} \frac{\hbar^2}{2m_e r_2^3} \sqrt{s(s+1)} \quad (100)$$

with the exceptions that the electric and magnetic forces are reduced by a factor of $\frac{1}{n}$ since the corresponding charge from Eq. (99) is $\frac{e}{n}$ and the magnetic force is further corrected by the factor of 2/3. With $s = \frac{1}{2}$,

$$r_2 = \left[n - \frac{\sqrt{3}}{3} \right] a_{He} \quad n = 2, 3, 4, \dots \quad (101)$$

The excited-state energy is the energy stored in the electric field, E_{ele} , given by Eq. (53) and Eqs. (1.232), (1.233), and (10.102) of Ref. [1] which is the energy of electron 2 relative to the ionized electron at rest having zero energy:

$$E_{ele} = -\frac{1}{n} \frac{e^2}{8\pi\epsilon_0 r_2} \quad (102)$$

where r_2 is given by Eq. (101) and from Eq. (99), $Z = 1/n$ in Eq. (53). The energies of the various singlet excited states of helium with $\ell = 0$ appear in Table 3.

As shown in the Special Relativistic Correction to the Ionization Energies section of Ref. [1] and Sec. IIDa the electron possesses an invariant charge-to-mass ratio ($\frac{e}{m_e}$) angular momentum of \hbar , and magnetic moment of a Bohr magneton (μ_B). *This invariance feature provides for the stability of multielectron atoms* as shown in the Two-Electron Atom section and

the Three, Four, Five, Six, Seven, Eight, Nine, Ten, Eleven, Twelve, Thirteen, Fourteen, Fifteen, Sixteen, Seventeen, Eighteen, Nineteen, and Twenty-Electron Atoms section of Ref. [1]. This feature also permits *the existence of excited states wherein electrons magnetically interact*. The electron's motion corresponds to a current which gives rise to a magnetic field with a field strength that is inversely proportional to its radius cubed as given in Eq. (100) wherein the magnetic field is a relativistic effect of the electric field as shown by Jackson [50]. Since the forces on electron 2 due to the nucleus and electron 1 (Eq. (100)) are radial/central, invariant of r_1 , and independent of r_1 with the condition that $r_1 < r_2$, r_2 can be determined without knowledge of r_1 . But, once r_2 is determined, r_1 can be solved using the equal and opposite magnetic force of electron 2 on electron 1 and the central Coulombic force corresponding to the nuclear charge of $2e$. Using Eq. (100), the force balance between the centrifugal and electric and magnetic forces is

$$\frac{m_e v^2}{r_1} = \frac{\hbar^2}{m_e r_1^3} = \frac{2e^2}{4\pi\epsilon_0 r_1^2} - \frac{1}{3n} \frac{\hbar^2}{m_e r_2^3} \sqrt{s(s+1)} \quad (103)$$

With $s = \frac{1}{2}$,

$$r_1^3 - \left(\frac{12n}{\sqrt{3}} r_2^3 \right) r_1 + \frac{6n}{\sqrt{3}} r_2^3 = 0 \quad n = 2, 3, 4, \dots \quad (104)$$

where r_2 is given by Eq. (101) and r_1 and r_2 are in units of a_{He} . To obtain the solution of cubic Eq. (104), let

$$g = \frac{6n}{\sqrt{3}} r_2^3 \quad (105)$$

Then, Eq. (104) becomes

$$r_1^3 - 2gr_1 + g = 0 \quad n = 2, 3, 4, \dots \quad (106)$$

and the roots are

$$r_{11} = A + B \quad (107)$$

$$r_{12} = -\frac{A+B}{2} + \frac{A-B}{2} \sqrt{-3} \quad (108)$$

$$r_{13} = -\frac{A+B}{2} - \frac{A-B}{2} \sqrt{-3} \quad (109)$$

where

$$A = \sqrt[3]{-\frac{g}{2} + \sqrt{\frac{g^2}{4} - \frac{8g^3}{27}}} = \sqrt[3]{\frac{g}{2}} \sqrt[3]{z} \quad (110)$$

and

$$B = \sqrt[3]{-\frac{g}{2} - \sqrt{\frac{g^2}{4} - \frac{8g^3}{27}}} = \sqrt[3]{\frac{g}{2}} \sqrt[3]{\bar{z}} \quad (111)$$

The complex number z is defined by

$$z = -1 + i\sqrt{\frac{32}{27}g - 1} = re^{i\theta} = r(\cos\theta + i\sin\theta) \quad (112)$$

where the modulus, r , and argument, θ , are

$$r = \sqrt{\frac{32}{27}g} \quad (113)$$

and

$$\theta = \frac{\pi}{2} + \sin^{-1}(1/r) \quad (114)$$

respectively. The cube roots are

$$\sqrt[3]{z} = \sqrt[3]{r}e^{i\theta/3} = \sqrt[3]{r}\left(\cos\frac{\theta}{3} + i\sin\frac{\theta}{3}\right) \quad (115)$$

$$\sqrt[3]{\bar{z}} = \sqrt[3]{r}e^{-i\theta/3} = \sqrt[3]{r}\left(\cos\frac{\theta}{3} - i\sin\frac{\theta}{3}\right) \quad (116)$$

So,

$$A = \sqrt[3]{\frac{g}{2}}r\left(\cos\frac{\theta}{3} + i\sin\frac{\theta}{3}\right) \quad (117)$$

and

$$B = \sqrt[3]{\frac{g}{2}}r\left(\cos\frac{\theta}{3} - i\sin\frac{\theta}{3}\right) \quad (118)$$

The real and physical root is

$$r_1 = r_{13} = -\sqrt{\frac{2}{3}}g\left(\cos\frac{\theta}{3} - \sqrt{3}\sin\frac{\theta}{3}\right) \quad (119)$$

B. Triplet Excited States with $\mathfrak{L} = \mathbf{0}$ ($1s^2 \rightarrow 1s^1(ns^1)$)

For the $\ell = 0$ singlet state, the time-averaged spin angular momentum of electron 2 is zero as given in Appendix VIII of Ref. [1]. A triplet state requires the further excitation to unpair the spin states of the two electrons. The angular momentum corresponding to the excited state is \hbar and the angular momentum change corresponding to the spin-flip is also \hbar as given in the Magnetic Parameters of the Electron (Bohr Magnetron) section of Ref. [1]. Then, the triplet state comprises spin interaction terms between the two electrons plus a contribution from the unpairing photon. As shown in the Resonant Precession of the Spin-1/2-Current-Density Function Gives Rise to the Bohr Magnetron section of Ref. [1], the electron spin angular momentum gives rise to a trapped photon with \hbar of angular momentum along an \mathbf{S} -axis. Then, the spin state of each of electron 1 and 2 comprises a photon standing wave that is phase-matched to a spherical harmonic source current, a spherical harmonic dipole $Y_\ell^m(\theta, \phi) = \sin\theta$ with respect to the \mathbf{S} -axis. The dipole spins about the \mathbf{S} -axis at the angular velocity given by Eq.(9) with \hbar of angular momentum. To conserve angular momentum, electron 2 rotates in the opposite direction about \mathbf{S} , the axis of the photon angular momentum due to the spin, and this rotation corresponds to $-\frac{2}{3}\hbar$ of angular momentum relative to \mathbf{S} . The corresponding angular momentum components of electron 2 due to spin, unpairing, and rotation are

$\mathbf{S} = \left(\sqrt{\frac{3}{4}}\hbar + \sqrt{\frac{3}{4}}\hbar - \frac{2}{3}\sqrt{\frac{3}{4}}\hbar \right) \mathbf{i}_z = \frac{4}{3}\sqrt{\frac{3}{4}}\hbar \mathbf{i}_z$ and $\mathbf{S} = \left(\frac{\hbar}{2} + \frac{\hbar}{2} - \frac{2}{3}\frac{\hbar}{2} \right) \mathbf{i}_z = \frac{4}{3}\frac{\hbar}{2} \mathbf{i}_z$. The corresponding angular momentum components of electron 1 are \hbar and $\sqrt{\frac{3}{4}}\hbar$, respectively. The magnetic interaction of each electron is equivalent to the magnetic field corresponding to a magnetic moment of μ_B interacting with an aligned magnetic momentum of $\frac{4}{3}\sqrt{\frac{3}{4}}\mu_B$. Since the triplet electron-electron interaction is twice that of the singlet case, the magnetic force for electron 2 is twice that of the singlet state as shown in Appendix VIII of Ref. [1]:

$$\frac{m_e v^2}{r_2} = \frac{\hbar^2}{m_e r_2^3} = \frac{1}{n} \frac{e^2}{4\pi\epsilon_0 r_2^2} + 2 \frac{2}{3} \frac{1}{n} \frac{\hbar^2}{2m_e r_2^3} \sqrt{s(s+1)} \quad (120)$$

With $s = \frac{1}{2}$,

$$r_2 = \left[n - \frac{2\sqrt{\frac{3}{4}}}{3} \right] a_{He} \quad n = 2, 3, 4, \dots \quad (121)$$

The excited-state energy is the energy stored in the electric field, E_{ele} , given by Eq. (102) where r_2 is given by Eq. (121). The energies of the various triplet excited states of helium with $\ell = 0$ appear in Table 4.

Using r_2 (Eq. (121)), r_1 can be solved using the equal and opposite magnetic force of electron 2 on electron 1 and the central Coulombic force corresponding to the nuclear charge of $2e$. Using Eq. (120), the force balance between the centrifugal and electric and magnetic forces is

$$\frac{m_e v^2}{r_1} = \frac{\hbar^2}{m_e r_1^3} = \frac{2e^2}{4\pi\epsilon_0 r_1^2} - \frac{2}{3n} \frac{\hbar^2}{m_e r_2^3} \sqrt{s(s+1)} \quad (122)$$

With $s = \frac{1}{2}$,

$$r_1^3 - \left(\frac{6n}{\sqrt{3}} r_2^3 \right) r_1 + \frac{3n}{\sqrt{3}} r_2^3 = 0 \quad n = 2, 3, 4, \dots \quad (123)$$

where r_2 is given by Eq. (121) and r_1 and r_2 are in units of a_{He} . To obtain the solution of cubic Eq. (123), let

$$g = \frac{3n}{\sqrt{3}} r_2^3 \quad (124)$$

Then, Eq. (123) becomes

$$r_1^3 - 2gr_1 + g = 0 \quad n = 2, 3, 4, \dots \quad (125)$$

Using Eqs. (106-119), the real and physical root is

$$r_1 = r_{13} = -\sqrt{\frac{2}{3}} g \left(\cos \frac{\theta}{3} - \sqrt{3} \sin \frac{\theta}{3} \right) \quad (126)$$

C. Singlet Excited States with $\ell \neq 0$

With $\ell \neq 0$, the electron source current in the excited state is the sum of constant and time-dependent functions where the latter, given by Eq. (15), travels about the z-axis. The current due to the time dependent term of Eq. (15) corresponding to p, d, f, etc. orbitals is given by Eq. (19). Jackson [42] gives the general multipole field solution to Maxwell's equations in a source-free region of empty space with the assumption of a time dependence $e^{i\omega_n t}$:

$$\begin{aligned}\mathbf{B} &= \sum_{\ell, m} \left[a_E(\ell, m) f_\ell(kr) \mathbf{X}_{\ell, m} - \frac{i}{k} a_M(\ell, m) \nabla \times g_\ell(kr) \mathbf{X}_{\ell, m} \right] \\ \mathbf{E} &= \sum_{\ell, m} \left[\frac{i}{k} a_E(\ell, m) \nabla \times f_\ell(kr) \mathbf{X}_{\ell, m} + a_M(\ell, m) g_\ell(kr) \mathbf{X}_{\ell, m} \right]\end{aligned}\quad (127)$$

where the cgs units used by Jackson are retained in this section. The radial functions $f_\ell(kr)$ and $g_\ell(kr)$ are of the form:

$$g_\ell(kr) = A_\ell^{(1)} h_\ell^{(1)} + A_\ell^{(2)} h_\ell^{(2)} \quad (128)$$

$\mathbf{X}_{\ell, m}$ is the vector spherical harmonic defined by

$$\mathbf{X}_{\ell, m}(\theta, \phi) = \frac{1}{\sqrt{\ell(\ell+1)}} \mathbf{L} Y_{\ell, m}(\theta, \phi) \quad (129)$$

where

$$\mathbf{L} = \frac{1}{i} (\mathbf{r} \times \nabla) \quad (130)$$

The coefficients $a_E(\ell, m)$ and $a_M(\ell, m)$ of Eq. (127) specify the amounts of electric (ℓ, m) multipole and magnetic (ℓ, m) multipole fields, and are determined by sources and boundary conditions as are the relative proportions in Eq. (128). Jackson gives the result of the electric and magnetic coefficients from the sources as

$$a_E(\ell, m) = \frac{4\pi k^2}{i\sqrt{\ell(\ell+1)}} \int Y_\ell^{m*} \left\{ \rho \frac{\delta}{\delta r} [r j_\ell(kr)] + \frac{ik}{c} (\mathbf{r} \cdot \mathbf{J}) j_\ell(kr) - ik \nabla \cdot (\mathbf{r} \times \mathbf{M}) j_\ell(kr) \right\} d^3 x \quad (131)$$

and

$$a_M(\ell, m) = \frac{-4\pi k^2}{\sqrt{\ell(\ell+1)}} \int j_\ell(kr) Y_\ell^{m*} \mathbf{L} \cdot \left(\frac{\mathbf{J}}{c} + \nabla \times \mathbf{M} \right) d^3 x \quad (132)$$

respectively, where the distribution of charge $\rho(\mathbf{x}, t)$, current $\mathbf{J}(\mathbf{x}, t)$, and intrinsic magnetization $\mathbf{M}(\mathbf{x}, t)$ are harmonically varying sources: $\rho(\mathbf{x})e^{-\omega_n t}$, $\mathbf{J}(\mathbf{x})e^{-\omega_n t}$, and $\mathbf{M}(\mathbf{x})e^{-\omega_n t}$. From Eq. (19), the charge and intrinsic magnetization terms are zero. Since the source dimensions are very small compared to a wavelength ($kr_{\max} \ll 1$), the small argument limit can be used to give the magnetic multipole coefficient $a_M(\ell, m)$ as

$$a_M(\ell, m) = \frac{-4\pi k^{\ell+2}}{(2\ell+1)!!} \left(\frac{\ell+1}{\ell}\right)^{1/2} (M_{\ell m} + M'_{\ell m}) = \frac{-4\pi k^{\ell+2}}{(2\ell+1)!} \left(\frac{\ell+1}{\ell}\right)^{1/2} (M_{\ell m} + M'_{\ell m}) \quad (133)$$

where the magnetic multipole moments are

$$M_{\ell m} = -\frac{1}{\ell+1} \int r^\ell Y_{\ell m}^* \nabla \cdot \left(\frac{\mathbf{r} \times \mathbf{J}}{c} \right) d^3x \quad (134)$$

$$M'_{\ell m} = -\int r^\ell Y_{\ell m}^* \nabla \cdot \mathbf{M} d^3x$$

From Eq. (1.108) of Ref. [1], the geometrical factor of the surface current-density function of the orbitsphere about the z-axis is $\left(\frac{2}{3}\right)^{-1}$. Using the geometrical factor, Eqs. (133-134), and Eqs. (16.101) and (16.102) of Jackson [51], the multipole coefficient $a_{Mag}(\ell, m)$ of the magnetic force of Eq. (60) is

$$a_{Mag}(\ell, m) = \frac{\frac{3}{2}}{(2\ell+1)!!} \frac{1}{\ell+2} \left(\frac{\ell+1}{\ell}\right)^{1/2} \quad (135)$$

For singlet states with $\ell \neq 0$, a minimum energy is achieved with conservation of the photon's angular momentum of \hbar when the magnetic moments of the corresponding angular momenta relative to the electron velocity (and corresponding Lorentzian forces given by Eq. (57)) superimpose negatively such that the spin component is radial (\mathbf{i}_r -direction) and the orbital component is central ($-\mathbf{i}_r$ -direction). The amplitude of the orbital angular momentum $\mathbf{L}_{rotational\ orbital}$, given by Eq. (43) is

$$\mathbf{L} = I\omega\mathbf{i}_z = \hbar \left[\frac{\ell(\ell+1)}{\ell^2 + 2\ell + 1} \right]^{1/2} = \hbar \sqrt{\frac{\ell}{\ell+1}} \quad (136)$$

Thus, using Eqs. (60), (99), and (135-136), the magnetic force between the two electrons given in Appendix VIII of Ref. [1] is

$$\mathbf{F}_{mag} = -\frac{1}{n} \frac{\frac{3}{2}}{(2\ell+1)!!} \frac{1}{\ell+2} \left(\frac{\ell+1}{\ell}\right)^{1/2} \frac{1}{2} \frac{\hbar^2}{m_e r^3} \left(\sqrt{s(s+1)} - \sqrt{\frac{\ell}{\ell+1}} \right) \quad (137)$$

and the force balance equation from Eq. (61) which achieves the condition that the sum of the mechanical momentum and electromagnetic momentum is conserved as given in Sections 6.6, 12.10, and 17.3 of Jackson [52] is

$$\frac{m_e v^2}{r_2} = \frac{\hbar^2}{m_e r_2^3} = \frac{1}{n} \frac{e^2}{4\pi\epsilon_0 r_2^2} - \frac{1}{n} \frac{\frac{3}{2}}{(2\ell+1)!!} \left(\frac{\ell+1}{\ell}\right)^{1/2} \frac{1}{\ell+2} \frac{1}{2} \frac{\hbar^2}{m_e r^3} \left(\sqrt{s(s+1)} - \sqrt{\frac{\ell}{\ell+1}} \right) \quad (138)$$

With $s = \frac{1}{2}$,

$$r_2 = \left[n + \frac{\frac{3}{4}}{(2\ell+1)!!} \frac{1}{\ell+2} \left(\frac{\ell+1}{\ell} \right)^{1/2} \left(\sqrt{\frac{3}{4}} - \sqrt{\frac{\ell}{\ell+1}} \right) \right] a_{He} \quad n = 2, 3, 4, \dots \quad (139)$$

The excited-state energy is the energy stored in the electric field, E_{ele} , given by Eq. (102) where r_2 is given by Eq. (139). The energies of the various singlet excited states of helium with $\ell \neq 0$ appear in Table 5.

Using r_2 (Eq. (139)), r_1 can be solved using the equal and opposite magnetic force of electron 2 on electron 1 and the central Coulombic force corresponding to the nuclear charge of $2e$. Using Eq. (138), the force balance between the centrifugal and electric and magnetic forces is

$$\frac{m_e v^2}{r_1} = \frac{\hbar^2}{m_e r_1^3} = \frac{2e^2}{4\pi\epsilon_0 r_1^2} + \frac{1}{n} \frac{\frac{3}{2}}{(2\ell+1)!!} \left(\frac{\ell+1}{\ell} \right)^{1/2} \frac{1}{\ell+2} \frac{1}{2} \frac{\hbar^2}{m_e r_2^3} \left(\sqrt{s(s+1)} - \sqrt{\frac{\ell}{\ell+1}} \right) \quad (140)$$

With $s = \frac{1}{2}$,

$$r_1^3 + \frac{n8r_1 r_2^3}{3 \left(\sqrt{\frac{3}{4}} - \sqrt{\frac{\ell}{\ell+1}} \right)} (2\ell+1)!! \left(\frac{\ell}{\ell+1} \right)^{1/2} (\ell+2) - \frac{n4r_2^3}{3 \left(\sqrt{\frac{3}{4}} - \sqrt{\frac{\ell}{\ell+1}} \right)} (2\ell+1)!! \left(\frac{\ell}{\ell+1} \right)^{1/2} (\ell+2) = 0 \quad n = 2, 3, 4, \dots \quad (141)$$

where r_2 is given by Eq. (139) and r_1 and r_2 are in units of a_{He} . To obtain the solution of cubic Eq. (141), let

$$g = - \frac{n4r_2^3}{3 \left(\sqrt{\frac{3}{4}} - \sqrt{\frac{\ell}{\ell+1}} \right)} (2\ell+1)!! \left(\frac{\ell}{\ell+1} \right)^{1/2} (\ell+2) \quad (142)$$

Then, Eq. (141) becomes

$$r_1^3 - 2gr_1 + g = 0 \quad n = 2, 3, 4, \dots \quad (143)$$

Three distinct cases arise depending on the value of ℓ . For $\ell = 1$ or $\ell = 2$, g of Eq. (142) is negative and A and B of Eqs. (110) and (111), respectively, are real:

$$A = \sqrt[3]{-\frac{g}{2}} \sqrt[3]{1 + \sqrt{1 - \frac{32}{27}g}} \quad (144)$$

and

$$B = -\sqrt[3]{-\frac{g}{2}} \sqrt[3]{\sqrt{1 - \frac{32}{27}g} - 1} \quad (145)$$

The only real root is

$$r_1 = r_{11} = \sqrt[3]{-\frac{g}{2}} \left\{ \sqrt[3]{1 + \sqrt{1 - \frac{32}{27}g}} - \sqrt[3]{1 - \frac{32}{27}g} - 1 \right\} \quad (146)$$

while r_{12} and r_{13} are complex conjugates. When $\ell = 3$ the magnetic force term (2nd term on RHS) of Eq. (138) is zero, and the force balance trivially gives

$$r_1 = 0.5a_{He} \quad (147)$$

When $\ell = 4, 5, 6, \dots$ all three roots are real, but, the physical root is r_{13} . In this case, note that $n \geq 5$, $\ell \geq 4$; so, the factor g of Eq. (142) is large ($> 10^8$). Expanding r_{13} for large values of g gives

$$r_1 = r_{13} = \frac{1}{2} + \frac{1}{16g} + O(g^{-3/2}) \quad (148)$$

D. Triplet Excited States with $\ell \neq 0$

For triplet states with $\ell \neq 0$, a minimum energy is achieved with conservation of the photon's angular momentum of \hbar when the magnetic moments of the corresponding angular momenta superimpose negatively such that the spin component is central and the orbital component is radial. Furthermore, as given for the triplet states with $\ell = 0$, the spin component in Eqs. (137) and (138) is doubled. Thus, the force balance equation given in Appendix VIII of Ref. [1] is

$$\frac{m_e v^2}{r_2} = \frac{\hbar^2}{m_e r_2^3} = \frac{1}{n} \frac{e^2}{4\pi\epsilon_0 r_2^2} + \frac{1}{n} \frac{\frac{3}{2}}{(2\ell+1)!!} \left(\frac{\ell+1}{\ell}\right)^{1/2} \frac{1}{\ell+2} \frac{1}{2} \frac{\hbar^2}{m_e r_2^3} \left(2\sqrt{s(s+1)} - \sqrt{\frac{\ell}{\ell+1}}\right) \quad (149)$$

With $s = \frac{1}{2}$,

$$r_2 = \left[n - \frac{\frac{3}{4}}{(2\ell+1)!!} \frac{1}{\ell+2} \left(\frac{\ell+1}{\ell}\right)^{1/2} \left(2\sqrt{\frac{3}{4}} - \sqrt{\frac{\ell}{\ell+1}}\right) \right] a_{He} \quad n = 2, 3, 4, \dots \quad (150)$$

The excited-state energy is the energy stored in the electric field, E_{ele} , given by Eq. (102) where r_2 is given by Eq. (150). The energies of the various triplet excited states of helium with $\ell \neq 0$ appear in Table 6. Using r_2 (Eq. (150)), r_1 can be solved using the equal and opposite magnetic force of electron 2 on electron 1 and the central Coulombic force corresponding to the nuclear charge of $2e$. Using Eq. (149), the force balance between the centrifugal and electric and magnetic forces is

$$\frac{m_e v^2}{r_1} = \frac{\hbar^2}{m_e r_1^3} = \frac{2e^2}{4\pi\epsilon_0 r_1^2} - \frac{1}{n} \frac{\frac{3}{2}}{(2\ell+1)!!} \left(\frac{\ell+1}{\ell}\right)^{1/2} \frac{1}{\ell+2} \frac{1}{2} \frac{\hbar^2}{m_e r_2^3} \left(2\sqrt{s(s+1)} - \sqrt{\frac{\ell}{\ell+1}}\right) \quad (151)$$

With $s = \frac{1}{2}$,

$$r_1^3 - \frac{n8r_1r_2^3}{3\left(\sqrt{\frac{3}{4}} - \sqrt{\frac{\ell}{\ell+1}}\right)}(2\ell+1)!!\left(\frac{\ell}{\ell+1}\right)^{1/2}(\ell+2) + \frac{n4r_2^3}{3\left(\sqrt{\frac{3}{4}} - \sqrt{\frac{\ell}{\ell+1}}\right)}(2\ell+1)!!\left(\frac{\ell}{\ell+1}\right)^{1/2}(\ell+2) = 0 \quad n = 2, 3, 4, \dots \quad (152)$$

where r_2 is given by Eq. (150) and r_1 and r_2 are in units of a_{He} . To obtain the solution of cubic Eq. (152), let

$$g = \frac{n4r_2^3}{3\left(\sqrt{\frac{3}{4}} - \sqrt{\frac{\ell}{\ell+1}}\right)}(2\ell+1)!!\left(\frac{\ell}{\ell+1}\right)^{1/2}(\ell+2) \quad (153)$$

Then, Eq. (152) becomes

$$r_1^3 - 2gr_1 + g = 0 \quad n = 2, 3, 4, \dots \quad (154)$$

Using Eqs. (106-119), the real and physical root is

$$r_1 = r_{13} = -\sqrt{\frac{2}{3}}g\left(\cos\frac{\theta}{3} - \sqrt{3}\sin\frac{\theta}{3}\right) \quad (155)$$

E. All Excited He I States

The combined energies of the various states of helium appear in Table 7. A plot of the predicted and experimental energies of levels assigned by NIST [19] appears in Figure 8. The spreadsheets to calculate the energies from exact solutions of all the excited states of the helium atom are available from the internet [27]. For over 100 measured states, the r-squared value is 0.999994, and the typical average relative difference is about 5 significant figures which is within the error of the experimental data. The agreement is remarkable.

F. Spin-Orbital Coupling of Excited States with $\ell \neq 0$

Due to 1.) the invariance of each of $\frac{e}{m_e}$ of the electron, the electron angular momentum of \hbar , and μ_B from the spin angular and orbital angular momentum, 2.) the condition that flux must be linked by the electron orbitsphere in units of the magnetic flux quantum, and 3.) the maximum projection of the spin angular momentum of the electron onto an axis is $\sqrt{\frac{3}{4}}\hbar$, the magnetic energy term of the electron g-factor gives the spin-orbital coupling energy $E_{s/o}$ (Eq. (2.102) of Ref. [1]):

$$E_{s/o} = 2 \frac{\alpha}{2\pi} \left(\frac{e\hbar}{2m_e} \right) \frac{\mu_0 e \hbar}{2(2\pi m_e) \left(\frac{r}{2\pi} \right)^3} \sqrt{\frac{3}{4}} = \frac{\alpha \pi \mu_0 e^2 \hbar^2}{m_e^2 r^3} \sqrt{\frac{3}{4}} \quad (156)$$

For the $n=2$ state of hydrogen, the radius is $r=2a_0$, and the predicted energy difference between the ${}^2P_{3/2}$ and ${}^2P_{1/2}$ levels of the hydrogen atom due to spin-orbital interaction is

$$E_{s/o} = \frac{\alpha \pi \mu_0 e^2 \hbar^2}{8m_e^2 a_0^3} \sqrt{\frac{3}{4}} \quad (157)$$

As in the case of the ${}^2P_{1/2} \rightarrow {}^2S_{1/2}$ transition, the photon-momentum transfer for the ${}^2P_{3/2} \rightarrow {}^2P_{1/2}$ transition gives rise to a small frequency shift derived after that of the Lamb shift with $\Delta m_\ell = -1$ included. The energy, E_{FS} , for the ${}^2P_{3/2} \rightarrow {}^2P_{1/2}$ transition called the fine structure splitting is given by Eq. (2.113) of Ref. [1]:

$$E_{FS} = \frac{\alpha^5 (2\pi)^2}{8} m_e c^2 \sqrt{\frac{3}{4}} + \left(13.5983 \text{ eV} \left(1 - \frac{1}{2^2} \right) \right)^2 \left[\frac{\left(\frac{3}{4\pi} \left(1 - \sqrt{\frac{3}{4}} \right) \right)^2}{2h\mu_e c^2} + \frac{\left(1 + \left(1 - \sqrt{\frac{3}{4}} \right) \right)^2}{2hm_H c^2} \right] \quad (158)$$

$$= 4.5190 \times 10^{-5} \text{ eV} + 1.75407 \times 10^{-7} \text{ eV}$$

$$= 4.53659 \times 10^{-5} \text{ eV}$$

where the first term corresponds to $E_{s/o}$ given by Eq. (157) expressed in terms of the mass energy of the electron (Eq. (2.106) of Ref. [1]) and the second and third terms correspond to the electron recoil and atom recoil, respectively. The energy of $4.53659 \times 10^{-5} \text{ eV}$ corresponds to a frequency of $10,969.4 \text{ MHz}$ or a wavelength of 2.73298 cm . The experimental value of the ${}^2P_{3/2} \rightarrow {}^2P_{1/2}$ transition frequency is $10,969.1 \text{ MHz}$. The large natural widths of the hydrogen $2p$ levels limits the experimental accuracy; yet, given this limitation, the agreement between the theoretical and experimental fine structure is excellent. Using r_2 given by Eq. (139), the spin-orbital energies were calculated for $\ell=1$ using Eq. (156) to compare to the effect of different ℓ quantum numbers. There is agreement between the magnitude of the predicted results given in Table 8 and the experimental dependence on the ℓ quantum number as given in Table 7.

V. Discussion

After decades of attempts to base quantum mechanics in reality, it is still purely mathematical [3, 8]. It is based on the postulate that the electron is a point with no volume with a vague probability wave requiring that the electron have multiple positions and energies including negative and infinite energies simultaneously. It may be time to revisit these 75 year old notions that 1.) fundamental particles such as the electron are one or zero dimensional and obey different physical laws than objects comprised of fundamental particles and 2.) the even

more disturbing view that fundamental particles don't obey physical laws—rather they obey mathematics devoid of physical laws. Perhaps mathematics does not determine physics. It only models physics.

It is true that the Schrödinger equation can be solved exactly for the hydrogen atom; although, it is not true that the result is the exact solution of the hydrogen atom. Spin and other parameters are missed entirely and there are many internal inconsistencies and nonphysical consequences that do not agree with experimental results [1-9]. The Dirac equation does not reconcile this situation [1-9]. Many additional shortcomings arise. Quantum mechanics is not a correct or complete theory of the physical world and inescapable internal inconsistencies and incongruities arise when attempts are made to treat it as a physical as opposed to a purely mathematical "tool". But, QM has severe limitations even as a tool. Beyond one-electron atoms, multielectron-atom quantum mechanical equations can not be solved except by approximation methods involving adjustable-parameter theories (perturbation theory, variational methods, self-consistent field method, multi-configuration Hartree Fock method, multi-configuration parametric potential method, $1/Z$ expansion method, multi-configuration Dirac-Fock method, electron correlation terms, QED terms, etc.)—all of which contain assumptions that can not be physically tested and are not consistent with physical laws.

The quantum mechanical "tool" even has progressively less utility in the case of scattering and excited states. Scattering models are not even truly quantum mechanical. The ionization of the bound electron does not give the required plane wave. Rather it is a sinusoidal point-particle-probability density function over all space. Similarly, the atomic scattering models can't be quantum mechanical, since it is trivial that the true four-point body scattering in the case of the helium atom utterly fails and disproves quantum mechanics. Calling the substitutes approximations is misleading. They are not approximations since they involve new physics or constructs such as the exact collinear alignment of the nucleus and the incident and atomic electrons or instantaneous action. In the case of the Born approximation, an average model that is not consistent with the Heisenberg Uncertainty Principle and special relativity is substituted for the true model, and even here the predictions do not match the data. In fact, it is reported that predictions "fail utterly at small scattering angles". Additional nonphysical adjustable-parameter or variational models having arbitrary accuracy are substituted at the expense of any physical meaning or relationship to any Schrödinger solution of the helium atom. They are simply curve fitting computer algorithms involving wave functions. Furthermore, neither the Schrödinger or Dirac equations can be solved for excited states; rather, new ad hoc trial-and-error algorithms are introduced that are not even consistent with the postulates of quantum mechanics. It is obvious from these issues that quantum mechanics based on the Schrödinger and Dirac equations fails at solving the helium atom just as the predecessor point-

particle theory of Bohr did. No consistency is achieved from the calculation of one parameter of helium to the next.

A theory of classical quantum mechanics (CQM) was derived from first principles that successfully applies physical laws on all scales [1-6]. The physical approach based on Maxwell's equations was previously applied to multielectron atoms that were solved exactly [1, 5]. The classical predictions of the ionization energies were solved for the physical electrons comprising concentric orbitspheres ("bubble-like" charge-density functions) that are electrostatic and magnetostatic corresponding to a constant charge distribution and a constant current corresponding to spin angular momentum. Alternatively, the charge is a superposition of a constant and a dynamical component. In the latter case, charge density waves on the surface are time and spherically harmonic and correspond additionally to electron orbital angular momentum that superimposes the spin angular momentum. Thus, the electrons of multielectron atoms all exist as orbitspheres of discrete radii which are given by r_n of the radial Dirac delta function, $\delta(r-r_n)$. These electron orbitspheres may be spin paired or unpaired depending on the force balance which applies to each electron. Ultimately, the electron configuration must be a minimum of energy. Minimum energy configurations are given by solutions to Laplace's equation. As demonstrated previously, this general solution also gives the functions of the resonant photons of excited states [1].

It was found that electrons of an atom with the same principal and l quantum numbers align parallel until each of the m_l levels are occupied, and then pairing occurs until each of the m_l levels contain paired electrons. The electron configuration for one through twenty-electron atoms that achieves an energy minimum is: $1s < 2s < 2p < 3s < 3p < 4s$. In each case, the corresponding force balance of the central Coulombic, paramagnetic, and diamagnetic forces was derived for each n -electron atom that was solved for the radius of each electron. The central Coulombic force was that of a point charge at the origin since the electron charge-density functions are spherically symmetrical with a time dependence that was nonradiative. This feature eliminated the electron-electron repulsion terms and the intractable infinities of quantum mechanics and permitted general solutions. The ionization energies were obtained using the calculated radii in the determination of the Coulombic and any magnetic energies. The radii and ionization energies for all cases were given by equations having fundamental constants and each nuclear charge, Z , only. The predicted ionization energies and electron configurations are in remarkable agreement with the experimental values known for 400 atoms and ions.

Using the solution for the helium atom, the elastic scattering of 500 eV electrons was derived using the predicted free electron corresponding to the $n = \infty$ state of the one-electron atom. The scattered electron intensity in the far field was given by the square of the amplitude

of the Fourier transform of the aperture function. The later was given by the convolution of the free, plane-wave electron with the helium atom orbitsphere. The corresponding Fourier transform integral reduces to a known lens formula that gives a curve that matches the data for all scattering angles.

In contrast to the shortcomings of quantum mechanics, with classical quantum mechanics (CQM), all excited states of the helium atom can be exactly solved in closed form. Photon absorption occurs by an excitation of a Maxwellian multipole cavity mode wherein the excitation is quantized according to the quantized energy and angular momentum of the photon given by $\hbar\omega$ and \hbar , respectively. The photon quantization causes the central electric-field corresponding the superimposed fields of the nucleus, electron 1, and the photon to be quantized and of magnitude of a reciprocal integer times that of the proton. This field and the phase-matched angular dependence of the trapped photon and excited-state electron as well as the spin orientation of the excited-state electron determine the central forces. The radii of electron 2 are determined from the force balance of the electric, magnetic, and centrifugal forces that corresponds to the minimum of energy of the system. Since the magnetic energies are relatively insignificant, the excited state energies are then given by *one physical term in each case, the Coulombic energy at the calculated radius*. Additional small terms may refine the predictions as discussed in the introduction to this Sec. IV; however, given the typical average relative difference is about 5 significant figures which is within the error of the experimental data, this result is remarkable and strongly confirms that the physical CQM solution of helium is correct.

All of the conjugate parameters are given using the same physical solution for the helium atom comprising a central alpha particle and two spin-paired orbitspheres at the same radius of $0.566987a_0$. The match between the theory and data confirm that this solution is accurate of the real, physical helium atom.

VI. Conclusion

Quantum mechanics fails the test for internal consistency with regard to the ionized electron, the ability to physically solve the helium atom, and predict both the ionization energy of helium and the correct scattering behavior of the free electrons as well as the excited states given any of the plethora of nonunique, nonphysical solutions. The adoption of the probabilistic versus deterministic nature of atomic particles violates all physical laws including special relativity with violation of causality as pointed out by Einstein [24] and de Broglie [53]. Consequently, it was rejected even by Schrödinger [54].

The Schrödinger and Dirac equations are not correct in that they do not represent reality as discussed in Sec. I. Thus, solutions of these equations involving any method are not correct even if they reproduce a number. This fact is confirmed in the case of the helium atom as given

in this paper. The mathematical quantum mechanical constructs are determined not to represent physical reality when it is demanded that the result of any given prediction is consistent with additional conjugate observables.

In contrast, the Maxwellian, exact orbitsphere model provides a continuous representation of all states of the electron including the ionized state as a plane wave having the de Broglie wavelength as given in the Electron in Free Space section of Ref. [1]. Using the exact, unique solution of the helium atom given in the Two-Electron Atom section of Ref. [1] and Sec. IIK, in a closed-form solution, the Maxwellian model predicts the experimental results of the electron scattering from helium for all angles as given in Sec. III. The solution of the helium atom is further proven to be correct since it is used to solve up through twenty-electron atoms in the Three, Four, Five, Six, Seven, Eight, Nine, Ten, Eleven, Twelve, Thirteen, Fifteen, Sixteen, Seventeen, Eighteen, Nineteen, and Twenty-Electron Atoms section of Ref [1] and over 100 excited-state energy levels in the Sec. IV. In the former case, the physical approach was applied to multielectron atoms that were solved exactly disproving the deep-seated view that such exact solutions can not exist according to quantum mechanics. The predictions from general solutions for one through twenty-electron atoms are in remarkable agreement with the experimental values known for 400 atoms and ions. In the latter case, the results given for any given n and ℓ quantum number in the equations agree remarkably well—up to 6 significant figures where the data is obtainable to that accuracy. These consistent results and the failure of the true quantum mechanical model as well as the unphysical Born approximation disprove the nature of the electron as a point particle which further disproves the primary assumption of quantum mechanics. The results directly prove that the electron is an extended particle and specifically show, in the case of the helium atom, that the electron function comprises two paired, electron orbitspheres at a radius given by Eqs. (62) and (80) as derived in the Two-Electron Atom section of Ref. [1] and Sec. IIK.

Since the quantum mechanical approaches of calculating ionization energies, scattering, and excited states of helium relies on arbitrary renormalization and adjustable parameters that can not be based on physics, they have no particular value outside of the computation exercise itself. They are meaningless numbers fitted and readjusted to match the most current observations. Thus, it can be argued that quantum mechanics gives correlations with experimental data. It does not explain the mechanism for the observed data. If you invoke the constraints of internal consistency and conformance to physical laws, quantum mechanics has not successfully solved the physical problem of the one or two-electron atom. In contrast, the presented exact physical solution for the helium atom implies that classical quantum mechanics is an accurate model of reality, and it is predictive which is not the case for quantum mechanics.

Acknowledgment

Special thanks to J. Webb for proposing the helium-excited-states problem and for researching the NIST energies and level assignments. Special thanks to M. Nansteel for working on the cubic equation solutions for helium excited states.

References

1. R. Mills, *The Grand Unified Theory of Classical Quantum Mechanics*, June 2006 Edition; posted at <http://www.blacklightpower.com/bookdownload.shtml>.
2. R. L. Mills, "The Grand Unified Theory of Classical Quantum Mechanics", *Int. J. Hydrogen Energy*, Vol. 27, No. 5, (2002), pp. 565-590.
3. R. L. Mills, "Classical Quantum Mechanics", *Physics Essays*, Vol. 16, No. 4, December, (2003), pp. 433-498.; posted at <http://www.blacklightpower.com/pdf/CQMTheoryPaperTablesand%20Figures080403.pdf>.
4. R. L. Mills, "The Nature of the Chemical Bond Revisited and an Alternative Maxwellian Approach", in press; posted at <http://www.blacklightpower.com/pdf/technical/H2PaperTableFiguresCaptions111303.pdf>.
5. R. L. Mills, "Exact Classical Quantum Mechanical Solutions for One- Through Twenty-Electron Atoms", in press; posted at <http://www.blacklightpower.com/pdf/technical/Exact%20Classical%20Quantum%20Mechanical%20Solutions%20for%20One-%20Through%20Twenty-Electron%20Atoms%20042204.pdf>.
6. R. L. Mills, "Maxwell's Equations and QED: Which is Fact and Which is Fiction", submitted; posted at <http://www.blacklightpower.com/pdf/technical/MaxwellianEquationsandQED080604.pdf>.
7. R. L. Mills, "The Fallacy of Feynman's Argument on the Stability of the Hydrogen Atom According to Quantum Mechanics", submitted; posted at <http://www.blacklightpower.com/pdf/Feynman%27s%20Argument%20Spec%20UPDATE%20091003.pdf>.
8. R. Mills, "The Nature of Free Electrons in Superfluid Helium--a Test of Quantum Mechanics and a Basis to Review its Foundations and Make a Comparison to Classical Theory", *Int. J. Hydrogen Energy*, Vol. 26, No. 10, (2001), pp. 1059-1096.
9. R. Mills, "The Hydrogen Atom Revisited", *Int. J. of Hydrogen Energy*, Vol. 25, Issue 12, December, (2000), pp. 1171-1183.
10. F. Laloë, Do we really understand quantum mechanics? Strange correlations, paradoxes, and theorems, *Am. J. Phys.* 69 (6), June 2001, 655-701.
11. H. Margenau, G. M. Murphy, *The Mathematics of Chemistry and Physics*, D. Van Nostrand

- Company, Inc., New York, (1943), pp. 363-367.
12. R. A. Bonham, M. Fink, *High Energy Electron Scattering*, ACS Monograph, Van Nostrand Reinhold Company, New York, (1974).
 13. P. J. Bromberg, "Absolute differential cross sections of elastically scattered electrons. I. He, N₂, and CO at 500 eV", *The Journal of Chemical Physics*, Vol. 50, No. 9, (1969), pp. 3906-3921.
 14. D. A. McQuarrie, *Quantum Chemistry*, University Science Books, Mill Valley, CA, (1983), p. 291.
 15. M. J. Brunger, S. J. Buckman, L. J. Allen, I. E. McCarthy, K. Ratnavelu, "Elastic electron scattering from helium: absolute experimental cross sections, theory and derived interaction potentials". *J. Phys. B: Opt. Phys.* Vol. 25, (1992), pp. 1823-1838.
 16. H. Margenau, G. M. Murphy, *The Mathematics of Chemistry and Physics*, D. Van Nostrand Company, Inc., New York, (1943), pp. 77-78.
 17. M. M. Waldrop, *Science*, Vol. 242, December, 2, (1988), pp. 1248-1250.
 18. B. Duan, X. -Y. Gu, Z. -Q. Ma, "Numerical calculation of energies of some excited states in a helium atom", *Eur. Phys. J. D*, Vol. 19, (2002), pp. 9-12.
 19. NIST Atomic Spectra Database, www.physics.nist.gov/cgi-bin/AtData/display.ksh.
 20. G. Landvogt, "The Grand Unified Theory of Classical Quantum Mechanics", *International Journal of Hydrogen Energy*, Vol. 28, No. 10, (2003), pp. 1155.
 21. P. Pearle, *Foundations of Physics*, "Absence of radiationless motions of relativistically rigid classical electron", Vol. 7, Nos. 11/12, (1977), pp. 931-945.
 22. V. F. Weisskopf, *Reviews of Modern Physics*, Vol. 21, No. 2, (1949), pp. 305-315.
 23. H. Wergeland, "The Klein Paradox Revisited", *Old and New Questions in Physics, Cosmology, Philosophy, and Theoretical Biology*, A. van der Merwe, Editor, Plenum Press, New York, (1983), pp. 503-515.
 24. A. Einstein, B. Podolsky, N. Rosen, *Phys. Rev.*, Vol. 47, (1935), p. 777.
 25. F. Dyson, "Feynman's proof of Maxwell equations", *Am. J. Phys.*, Vol. 58, (1990), pp. 209-211.
 26. H. A. Haus, "On the radiation from point charges", *American Journal of Physics*, Vol. 54, 1126-1129 (1986).
 27. <http://www.blacklightpower.com/new.shtml>.
 28. D. A. McQuarrie, *Quantum Chemistry*, University Science Books, Mill Valley, CA, (1983), pp. 206-225.
 29. J. Daboul and J. H. D. Jensen, *Z. Physik*, Vol. 265, (1973), pp. 455-478.
 30. T. A. Abbott and D. J. Griffiths, *Am. J. Phys.*, Vol. 53, No. 12, (1985), pp. 1203-1211.
 31. G. Goedecke, *Phys. Rev* 135B, (1964), p. 281.

32. D. A. McQuarrie, *Quantum Chemistry*, University Science Books, Mill Valley, CA, (1983), pp. 238-241.
33. R. S. Van Dyck, Jr., P. Schwinberg, H. Dehmelt, "New high precision comparison of electron and positron g factors", *Phys. Rev. Lett.*, Vol. 59, (1987), p. 26-29.
34. C. E. Moore, "Ionization Potentials and Ionization Limits Derived from the Analyses of Optical Spectra, Nat. Stand. Ref. Data Ser.-Nat. Bur. Stand. (U.S.), No. 34, 1970.
35. R. C. Weast, *CRC Handbook of Chemistry and Physics*, 58 Edition, CRC Press, West Palm Beach, Florida, (1977), p. E-68.
36. J. D. Jackson, *Classical Electrodynamics*, Second Edition, John Wiley & Sons, New York, (1975), pp. 236-240, 601-608, 786-790.
37. http://physics.nist.gov/PhysRefData/ASD/levels_form.html.
38. A. Gumberidze, Th. Stöhlker, D. Banas, K. Beckert, P. Beller, H. F. Beyer, F. Bosch, S. Hagmann, C. Kozhuharov, D. Liesen, F. Nolden, X. Ma, P.H. Mokler, M. Steck, D. Sierpowski, and S. Tashenov, "Quantum electrodynamics in strong electric fields: The ground-state Lamb shift in hydrogenlike uranium," *Phys. Rev. Letts.*, Vol. 94, 223001 (2005).
39. E. M. Purcell, *Electricity and Magnetism*, McGraw-Hill, New York, (1985), Second Edition, pp. 451-458.
40. G. O. Reynolds, J. B. DeVelis, G. B. Parrent, B. J. Thompson, *The New Physical Optics Notebook*, SPIE Optical Engineering Press, (1990).
41. R. A. Bonham, M. Fink, *High Energy Electron Scattering*, ACS Monograph, Van Nostrand Reinhold Company, New York, (1974), pp. 1-3.
42. J. D. Jackson, *Classical Electrodynamics*, Second Edition, John Wiley & Sons, New York, (1975), pp. 739-779.
43. R. N. Bracewell, *The Fourier Transform and Its Applications*, McGraw-Hill Book Company, New York, (1978), pp. 252-253.
44. A. Apelblat, *Table of Definite and Infinite Integrals*, Elsevier Scientific Publishing Company, Amsterdam, (1983).
45. P. J. Bromberg, "Absolute differential cross sections of elastically scattered electrons. I. He, N₂, and CO at 500 eV", *The Journal of Chemical Physics*, Vol. 50, No. 9, (1969), pp. 3906-3921.
46. J. Geiger, "Elastische und unelastische streuung von elektronen an gasen", *Zeitschrift für Physik*, Vol. 175, (1963), pp. 530-542.
47. F. Bueche, *Introduction to Physics for Scientists and Engineers*, McGraw-Hill, (1975), pp. 352-353.
48. M. Mizushima, *Quantum Mechanics of Atomic Spectra and Atomic Structure*, W.A. Benjamin, Inc., New York, (1970), p.17.

49. J. D. Jackson, *Classical Electrodynamics*, Second Edition, John Wiley & Sons, New York, (1975), pp. 747-752.
50. J. D. Jackson, *Classical Electrodynamics*, Second Edition, John Wiley & Sons, New York, (1975), pp. 503-561.
51. J. D. Jackson, *Classical Electrodynamics*, Second Edition, John Wiley & Sons, New York, (1975), p. 759.
52. J. D. Jackson, *Classical Electrodynamics*, Second Edition, John Wiley & Sons, New York, (1975), pp. 236-240, 601-608, 786-790.
53. L. de Broglie, "On the true ideas underlying wave mechanics", *Old and New Questions in Physics, Cosmology, Philosophy, and Theoretical Biology*, A. van der Merwe, Editor, Plenum Press, New York, (1983), pp. 83-86.
54. D. C. Cassidy, *Uncertainty the Life and Science of Werner Heisenberg*, W. H. Freeman and Company, New York, (1992), pp. 224-225.

Table 1. Relativistic ionization energies for some one-electron atoms.

One e Atom	Z	β (Eq. (1.267) of Ref. [7])	Theoretical Ionization Energies (eV) (Eq. (1.272) of Ref. [7])	Experimental Ionization Energies (eV) ^a	Relative Difference between Experimental and Calculated ^b
<i>H</i>	1	0.00730	13.59847	13.59844	-0.000002
<i>He</i> ⁺	2	0.01459	54.41826	54.41778	-0.000009
<i>Li</i> ²⁺	3	0.02189	122.45637	122.45429	-0.000017
<i>Be</i> ³⁺	4	0.02919	217.72427	217.71865	-0.000026
<i>B</i> ⁴⁺	5	0.03649	340.23871	340.2258	-0.000038
<i>C</i> ⁵⁺	6	0.04378	490.01759	489.99334	-0.000049
<i>N</i> ⁶⁺	7	0.05108	667.08834	667.046	-0.000063
<i>O</i> ⁷⁺	8	0.05838	871.47768	871.4101	-0.000078
<i>F</i> ⁸⁺	9	0.06568	1103.220	1103.1176	-0.000093
<i>Ne</i> ⁹⁺	10	0.07297	1362.348	1362.1995	-0.000109
<i>Na</i> ¹⁰⁺	11	0.08027	1648.910	1648.702	-0.000126
<i>Mg</i> ¹¹⁺	12	0.08757	1962.945	1962.665	-0.000143
<i>Al</i> ¹²⁺	13	0.09486	2304.512	2304.141	-0.000161
<i>Si</i> ¹³⁺	14	0.10216	2673.658	2673.182	-0.000178
<i>P</i> ¹⁴⁺	15	0.10946	3070.451	3069.842	-0.000198
<i>S</i> ¹⁵⁺	16	0.11676	3494.949	3494.1892	-0.000217
<i>Cl</i> ¹⁶⁺	17	0.12405	3947.228	3946.296	-0.000236
<i>Ar</i> ¹⁷⁺	18	0.13135	4427.363	4426.2296	-0.000256
<i>K</i> ¹⁸⁺	19	0.13865	4935.419	4934.046	-0.000278
<i>Ca</i> ¹⁹⁺	20	0.14595	5471.494	5469.864	-0.000298
<i>Sc</i> ²⁰⁺	21	0.15324	6035.681	6033.712	-0.000326
<i>Ti</i> ²¹⁺	22	0.16054	6628.064	6625.82	-0.000339
<i>V</i> ²²⁺	23	0.16784	7248.745	7246.12	-0.000362
<i>Cr</i> ²³⁺	24	0.17514	7897.827	7894.81	-0.000382
<i>Mn</i> ²⁴⁺	25	0.18243	8575.426	8571.94	-0.000407
<i>Fe</i> ²⁵⁺	26	0.18973	9281.650	9277.69	-0.000427
<i>Co</i> ²⁶⁺	27	0.19703	10016.63	10012.12	-0.000450
<i>Ni</i> ²⁷⁺	28	0.20432	10780.48	10775.4	-0.000471
<i>Cu</i> ²⁸⁺	29	0.21162	11573.34	11567.617	-0.000495
<i>Zn</i> ²⁹⁺	30	0.21892	12395.35	12388.93	-0.000518
<i>Ga</i> ³⁰⁺	31	0.22622	13246.66	13239.49	-0.000542
<i>Ge</i> ³¹⁺	32	0.23351	14127.41	14119.43	-0.000565

<i>As</i> ³²⁺	33	0.24081	15037.75	15028.62	-0.000608
<i>Se</i> ³³⁺	34	0.24811	15977.86	15967.68	-0.000638
<i>Kr</i> ³⁵⁺	36	0.26270	17948.05	17936.21	-0.000660
<i>Rb</i> ³⁶⁺	37	0.27000	18978.49	18964.99	-0.000712
<i>Mo</i> ⁴¹⁺	42	0.30649	24592.04	24572.22	-0.000807
<i>Xe</i> ⁵³⁺	54	0.39406	41346.76	41299.7	-0.001140
<i>U</i> ⁹¹⁺	92	0.67136	132279.32	131848.5	-0.003268

^a From theoretical calculations, interpolation of H isoelectronic and Rydberg series, and experimental data [34-37].

^b (Experimental-theoretical)/experimental.

Table 2. Relativistically corrected ionization energies for some two-electron atoms.

2 e Atom	Z	r_1 (a_0) ^a	Electric Energy ^b (eV)	Magnetic Energy ^c (eV)	Velocity (m/s) ^d	γ^* ^e	Theoretical Ionization Energies ^f (eV)	Experimental Ionization Energies ^g (eV)	Relative Error ^h
He	2	0.566987	23.996467	0.590536	3.85845E+06	1.000021	24.58750	24.58741	-0.000004
Li ⁺	3	0.35566	76.509	2.543	6.15103E+06	1.00005	75.665	75.64018	-0.0003
Be ²⁺	4	0.26116	156.289	6.423	8.37668E+06	1.00010	154.699	153.89661	-0.0052
B ³⁺	5	0.20670	263.295	12.956	1.05840E+07	1.00016	260.746	259.37521	-0.0053
C ⁴⁺	6	0.17113	397.519	22.828	1.27836E+07	1.00024	393.809	392.087	-0.0044
N ⁵⁺	7	0.14605	558.958	36.728	1.49794E+07	1.00033	553.896	552.0718	-0.0033
O ⁶⁺	8	0.12739	747.610	55.340	1.71729E+07	1.00044	741.023	739.29	-0.0023
F ⁷⁺	9	0.11297	963.475	79.352	1.93649E+07	1.00057	955.211	953.9112	-0.0014
Ne ⁸⁺	10	0.10149	1206.551	109.451	2.15560E+07	1.00073	1196.483	1195.8286	-0.0005
Na ⁹⁺	11	0.09213	1476.840	146.322	2.37465E+07	1.00090	1464.871	1465.121	0.0002
Mg ¹⁰⁺	12	0.08435	1774.341	190.652	2.59364E+07	1.00110	1760.411	1761.805	0.0008
Al ¹¹⁺	13	0.07778	2099.05	243.13	2.81260E+07	1.00133	2083.15	2085.98	0.0014
Si ¹²⁺	14	0.07216	2450.98	304.44	3.03153E+07	1.00159	2433.13	2437.63	0.0018
P ¹³⁺	15	0.06730	2830.11	375.26	3.25043E+07	1.00188	2810.42	2816.91	0.0023
S ¹⁴⁺	16	0.06306	3236.46	456.30	3.46932E+07	1.00221	3215.09	3223.78	0.0027
Cl ¹⁵⁺	17	0.05932	3670.02	548.22	3.68819E+07	1.00258	3647.22	3658.521	0.0031
Ar ¹⁶⁺	18	0.05599	4130.79	651.72	3.90705E+07	1.00298	4106.91	4120.8857	0.0034
K ¹⁷⁺	19	0.05302	4618.77	767.49	4.12590E+07	1.00344	4594.25	4610.8	0.0036
Ca ¹⁸⁺	20	0.05035	5133.96	896.20	4.34475E+07	1.00394	5109.38	5128.8	0.0038
Sc ¹⁹⁺	21	0.04794	5676.37	1038.56	4.56358E+07	1.00450	5652.43	5674.8	0.0039
Ti ²⁰⁺	22	0.04574	6245.98	1195.24	4.78241E+07	1.00511	6223.55	6249	0.0041
V ²¹⁺	23	0.04374	6842.81	1366.92	5.00123E+07	1.00578	6822.93	6851.3	0.0041
Cr ²²⁺	24	0.04191	7466.85	1554.31	5.22005E+07	1.00652	7450.76	7481.7	0.0041
Mn ²³⁺	25	0.04022	8118.10	1758.08	5.43887E+07	1.00733	8107.25	8140.6	0.0041
Fe ²⁴⁺	26	0.03867	8796.56	1978.92	5.65768E+07	1.00821	8792.66	8828	0.0040
Co ²⁵⁺	27	0.03723	9502.23	2217.51	5.87649E+07	1.00917	9507.25	9544.1	0.0039
Ni ²⁶⁺	28	0.03589	10235.12	2474.55	6.09529E+07	1.01022	10251.33	10288.8	0.0036
Cu ²⁷⁺	29	0.03465	10995.21	2750.72	6.31409E+07	1.01136	11025.21	11062.38	0.0034

^a From Eq. (62).

^b From Eq. (64).

^c From Eq. (65).

^d From Eq. (67).

^e From Eq. (1.250) of Ref. [1] (follows Eqs. (6), (16), and (49)) with the velocity given by Eq. (67).

^f From Eqs. (63) and (66) with $E(\text{electric})$ of Eq. (64) relativistically corrected by γ^* according to Eq.(1.251) of Ref. [1] except that the electron-nuclear electrodynamic relativistic factor corresponding to the reduced mass of Eqs. (1.213-1.223) was not included.

^g From theoretical calculations for ions Ne⁸⁺ and Cu²⁸⁺ [34,35].

^h (Experimental-theoretical)/experimental.

Table 3. Calculated and experimental energies of He I singlet excited states with $\ell = 0$ ($1s^2 \rightarrow 1s^1(ns^1)$).

n	r_1 (a_{He}) ^a	r_2 (a_{He}) ^b	Term Symbol	E_{ele} CQM He I Energy Levels ^c (eV)	NIST He I Energy Levels ^d (eV)	Difference CQM-NIST (eV)	Relative Difference ^e (CQM- NIST)
2	0.501820	1.71132	1s2s ¹ S	-3.97465	-3.97161	-0.00304	0.00077
3	0.500302	2.71132	1s3s ¹ S	-1.67247	-1.66707	-0.00540	0.00324
4	0.500088	3.71132	1s4s ¹ S	-0.91637	-0.91381	-0.00256	0.00281
5	0.500035	4.71132	1s5s ¹ S	-0.57750	-0.57617	-0.00133	0.00230
6	0.500016	5.71132	1s6s ¹ S	-0.39698	-0.39622	-0.00076	0.00193
7	0.500009	6.71132	1s7s ¹ S	-0.28957	-0.2891	-0.00047	0.00163
8	0.500005	7.71132	1s8s ¹ S	-0.22052	-0.2202	-0.00032	0.00144
9	0.500003	8.71132	1s9s ¹ S	-0.17351	-0.1733	-0.00021	0.00124
10	0.500002	9.71132	1s10s ¹ S	-0.14008	-0.13992	-0.00016	0.00116
11	0.500001	10.71132	1s11s ¹ S	-0.11546	-0.11534	-0.00012	0.00103
Avg.						-0.00144	0.00175

^a Radius of the inner electron 1 from Eq. (119).

^b Radius of the outer electron 2 from Eq. (101).

^c Classical quantum mechanical (CQM) calculated energy levels given by the electric energy (Eq. (102)).

^d Experimental NIST levels [19] with the ionization potential defined as zero.

^e (Theoretical-Experimental)/Experimental.

Table 4. Calculated and experimental energies of He I triplet excited states with $\ell = 0$ ($1s^2 \rightarrow 1s^1(ns^1)$).

n	r_1 (a_{He}) ^a	r_2 (a_{He}) ^b	Term Symbol	E_{ele} CQM He I Energy Levels ^c (eV)	NIST He I Energy Levels ^d (eV)	Difference CQM-NIST (eV)	Relative Difference ^e (CQM- NIST)
2	0.506514	1.42265	1s2s ³ S	-4.78116	-4.76777	-0.01339	0.00281
3	0.500850	2.42265	1s3s ³ S	-1.87176	-1.86892	-0.00284	0.00152
4	0.500225	3.42265	1s4s ³ S	-0.99366	-0.99342	-0.00024	0.00024
5	0.500083	4.42265	1s5s ³ S	-0.61519	-0.61541	0.00022	-0.00036
6	0.500038	5.42265	1s6s ³ S	-0.41812	-0.41838	0.00026	-0.00063
7	0.500019	6.42265	1s7s ³ S	-0.30259	-0.30282	0.00023	-0.00077
8	0.500011	7.42265	1s8s ³ S	-0.22909	-0.22928	0.00019	-0.00081
9	0.500007	8.42265	1s9s ³ S	-0.17946	-0.17961	0.00015	-0.00083
10	0.500004	9.42265	1s10s ³ S	-0.14437	-0.14445	0.00013	-0.00087
11	0.500003	10.42265	1s11s ³ S	-0.11866	-0.11876	0.00010	-0.00087
					Avg.	-0.00152	-0.00006

^a Radius of the inner electron 1 from Eq. (126).

^b Radius of the outer electron 2 from Eq. (121).

^c Classical quantum mechanical (CQM) calculated energy levels given by the electric energy (Eq. (102)).

^d Experimental NIST levels [19] with the ionization potential defined as zero.

^e (Theoretical-Experimental)/Experimental.

Table 5. Calculated and experimental energies of He I singlet excited states with $\ell \neq 0$.

n	ℓ	r_1 (a_{He}) ^a	r_2 (a_{He}) ^b	Term Symbol	E_{ele} CQM He I Energy Levels ^c (eV)	NIST He I Energy Levels ^d (eV)	Difference CQM-NIST (eV)	Relative Difference ^e (CQM-NIST)
2	1	0.499929	2.01873	1s2p ¹ P ⁰	-3.36941	-3.36936	-0.0000477	0.0000141
3	2	0.499999	3.00076	1s3d ¹ D	-1.51116	-1.51331	0.0021542	-0.0014235
3	1	0.499986	3.01873	1s3p ¹ P ⁰	-1.50216	-1.50036	-0.0017999	0.0011997
4	2	0.500000	4.00076	1s4d ¹ D	-0.85008	-0.85105	0.0009711	-0.0011411
4	3	0.500000	4.00000	1s4f ¹ F ⁰	-0.85024	-0.85037	0.0001300	-0.0001529
4	1	0.499995	4.01873	1s4p ¹ P ⁰	-0.84628	-0.84531	-0.0009676	0.0011446
5	2	0.500000	5.00076	1s5d ¹ D	-0.54407	-0.54458	0.0005089	-0.0009345
5	3	0.500000	5.00000	1s5f ¹ F ⁰	-0.54415	-0.54423	0.0000764	-0.0001404
5	4	0.500000	5.00000	1s5g ¹ G	-0.54415	-0.54417	0.0000159	-0.0000293
5	1	0.499998	5.01873	1s5p ¹ P ⁰	-0.54212	-0.54158	-0.0005429	0.0010025
6	2	0.500000	6.00076	1s6d ¹ D	-0.37784	-0.37813	0.0002933	-0.0007757
6	3	0.500000	6.00000	1s6f ¹ F ⁰	-0.37788	-0.37793	0.0000456	-0.0001205
6	4	0.500000	6.00000	1s6g ¹ G	-0.37788	-0.37789	0.0000053	-0.0000140
6	5	0.500000	6.00000	1s6h ¹ H ⁰	-0.37788	-0.37788	-0.0000045	0.0000119
6	1	0.499999	6.01873	1s6p ¹ P ⁰	-0.37671	-0.37638	-0.0003286	0.0008730
7	2	0.500000	7.00076	1s7d ¹ D	-0.27760	-0.27779	0.0001907	-0.0006864
7	3	0.500000	7.00000	1s7f ¹ F ⁰	-0.27763	-0.27766	0.0000306	-0.0001102
7	4	0.500000	7.00000	1s7g ¹ G	-0.27763	-0.27763	0.0000004	-0.0000016
7	5	0.500000	7.00000	1s7h ¹ H ⁰	-0.27763	-0.27763	0.0000006	-0.0000021
7	6	0.500000	7.00000	1s7i ¹ I	-0.27763	-0.27762	-0.0000094	0.0000338
7	1	0.500000	7.01873	1s7p ¹ P ⁰	-0.27689	-0.27667	-0.0002186	0.0007900
					Avg.		0.0000240	-0.0000220

^a Radius of the inner electron 1 from Eq. (146) for $\ell = 1$ or $\ell = 2$, Eq. (147) for $\ell = 3$, and Eq. (148) for $\ell = 4, 5, 6, \dots$.

^b Radius of the outer electron 2 from Eq. (139).

^c Classical quantum mechanical (CQM) calculated energy levels given by the electric energy (Eq. (102)).

^d Experimental NIST levels [19] with the ionization potential defined as zero.

^e (Theoretical-Experimental)/Experimental.

Table 6. Calculated and experimental energies of He I triplet excited states with $\ell \neq 0$.

n	ℓ	r_1 (a_{He}) ^a	r_2 (a_{He}) ^b	Term Symbol	E_{ele} CQM He I Energy Levels ^c (eV)	NIST He I Energy Levels ^d (eV)	Difference CQM-NIST (eV)	Relative Difference ^e (CQM-NIST)
2	1	0.500571	1.87921	1s2p $^3P_2^0$	-3.61957	-3.6233	0.0037349	-0.0010308
2	1	0.500571	1.87921	1s2p $^3P_1^0$	-3.61957	-3.62329	0.0037249	-0.0010280
2	1	0.500571	1.87921	1s2p $^3P_0^0$	-3.61957	-3.62317	0.0036049	-0.0009949
3	1	0.500105	2.87921	1s3p $^3P_2^0$	-1.57495	-1.58031	0.0053590	-0.0033911
3	1	0.500105	2.87921	1s3p $^3P_1^0$	-1.57495	-1.58031	0.0053590	-0.0033911
3	1	0.500105	2.87921	1s3p $^3P_0^0$	-1.57495	-1.58027	0.0053190	-0.0033659
3	2	0.500011	2.98598	1s3d 3D_3	-1.51863	-1.51373	-0.0049031	0.0032391
3	2	0.500011	2.98598	1s3d 3D_2	-1.51863	-1.51373	-0.0049031	0.0032391
3	2	0.500011	2.98598	1s3d 3D_1	-1.51863	-1.51373	-0.0049031	0.0032391
4	1	0.500032	3.87921	1s4p $^3P_2^0$	-0.87671	-0.87949	0.0027752	-0.0031555
4	1	0.500032	3.87921	1s4p $^3P_1^0$	-0.87671	-0.87949	0.0027752	-0.0031555
4	1	0.500032	3.87921	1s4p $^3P_0^0$	-0.87671	-0.87948	0.0027652	-0.0031442
4	2	0.500003	3.98598	1s4d 3D_3	-0.85323	-0.85129	-0.0019398	0.0022787
4	2	0.500003	3.98598	1s4d 3D_2	-0.85323	-0.85129	-0.0019398	0.0022787
4	2	0.500003	3.98598	1s4d 3D_1	-0.85323	-0.85129	-0.0019398	0.0022787
4	3	0.500000	3.99857	1s4f $^3F_3^0$	-0.85054	-0.85038	-0.0001638	0.0001926
4	3	0.500000	3.99857	1s4f $^3F_4^0$	-0.85054	-0.85038	-0.0001638	0.0001926
4	3	0.500000	3.99857	1s4f $^3F_2^0$	-0.85054	-0.85038	-0.0001638	0.0001926
5	1	0.500013	4.87921	1s5p $^3P_2^0$	-0.55762	-0.55916	0.0015352	-0.0027456
5	1	0.500013	4.87921	1s5p $^3P_1^0$	-0.55762	-0.55916	0.0015352	-0.0027456
5	1	0.500013	4.87921	1s5p $^3P_0^0$	-0.55762	-0.55915	0.0015252	-0.0027277
5	2	0.500001	4.98598	1s5d 3D_3	-0.54568	-0.54472	-0.0009633	0.0017685
5	2	0.500001	4.98598	1s5d 3D_2	-0.54568	-0.54472	-0.0009633	0.0017685
5	2	0.500001	4.98598	1s5d 3D_1	-0.54568	-0.54472	-0.0009633	0.0017685
5	3	0.500000	4.99857	1s5f $^3F_3^0$	-0.54431	-0.54423	-0.0000791	0.0001454
5	3	0.500000	4.99857	1s5f $^3F_4^0$	-0.54431	-0.54423	-0.0000791	0.0001454
5	3	0.500000	4.99857	1s5f $^3F_2^0$	-0.54431	-0.54423	-0.0000791	0.0001454
5	4	0.500000	4.99988	1s5g 3G_4	-0.54417	-0.54417	0.0000029	-0.0000054
5	4	0.500000	4.99988	1s5g 3G_5	-0.54417	-0.54417	0.0000029	-0.0000054

5	4	0.500000	4.99988	1s5g 3G_3	-0.54417	-0.54417	0.0000029	-0.0000054
6	1	0.500006	5.87921	1s6p $^3P_2^0$	-0.38565	-0.38657	0.0009218	-0.0023845
6	1	0.500006	5.87921	1s6p $^3P_1^0$	-0.38565	-0.38657	0.0009218	-0.0023845
6	1	0.500006	5.87921	1s6p $^3P_0^0$	-0.38565	-0.38657	0.0009218	-0.0023845
6	2	0.500001	5.98598	1s6d 3D_3	-0.37877	-0.37822	-0.0005493	0.0014523
6	2	0.500001	5.98598	1s6d 3D_2	-0.37877	-0.37822	-0.0005493	0.0014523
6	2	0.500001	5.98598	1s6d 3D_1	-0.37877	-0.37822	-0.0005493	0.0014523
6	3	0.500000	5.99857	1s6f $^3F_3^0$	-0.37797	-0.37793	-0.0000444	0.0001176
6	3	0.500000	5.99857	1s6f $^3F_4^0$	-0.37797	-0.37793	-0.0000444	0.0001176
6	3	0.500000	5.99857	1s6f $^3F_2^0$	-0.37797	-0.37793	-0.0000444	0.0001176
6	4	0.500000	5.99988	1s6g 3G_4	-0.37789	-0.37789	-0.0000023	0.0000060
6	4	0.500000	5.99988	1s6g 3G_5	-0.37789	-0.37789	-0.0000023	0.0000060
6	4	0.500000	5.99988	1s6g 3G_3	-0.37789	-0.37789	-0.0000023	0.0000060
6	5	0.500000	5.99999	1s6h $^3H_4^0$	-0.37789	-0.37788	-0.0000050	0.0000133
6	5	0.500000	5.99999	1s6h $^3H_5^0$	-0.37789	-0.37788	-0.0000050	0.0000133
6	5	0.500000	5.99999	1s6h $^3H_6^0$	-0.37789	-0.37788	-0.0000050	0.0000133
7	1	0.500003	6.87921	1s7p $^3P_2^0$	-0.28250	-0.28309	0.0005858	-0.0020692
7	1	0.500003	6.87921	1s7p $^3P_1^0$	-0.28250	-0.28309	0.0005858	-0.0020692
7	1	0.500003	6.87921	1s7p $^3P_0^0$	-0.28250	-0.28309	0.0005858	-0.0020692
7	2	0.500000	6.98598	1s7d 3D_3	-0.27819	-0.27784	-0.0003464	0.0012468
7	2	0.500000	6.98598	1s7d 3D_2	-0.27819	-0.27784	-0.0003464	0.0012468
7	2	0.500000	6.98598	1s7d 3D_1	-0.27819	-0.27784	-0.0003464	0.0012468
7	3	0.500000	6.99857	1s7f $^3F_3^0$	-0.27769	-0.27766	-0.0000261	0.0000939
7	3	0.500000	6.99857	1s7f $^3F_4^0$	-0.27769	-0.27766	-0.0000261	0.0000939
7	3	0.500000	6.99857	1s7f $^3F_2^0$	-0.27769	-0.27766	-0.0000261	0.0000939
7	4	0.500000	6.99988	1s7g 3G_4	-0.27763	-0.27763	-0.0000043	0.0000155
7	4	0.500000	6.99988	1s7g 3G_5	-0.27763	-0.27763	-0.0000043	0.0000155
7	4	0.500000	6.99988	1s7g 3G_3	-0.27763	-0.27763	-0.0000043	0.0000155
7	5	0.500000	6.99999	1s7h $^3H_5^0$	-0.27763	-0.27763	0.0000002	-0.0000009

7	5	0.500000	6.99999	1s7h $^3\text{H}_6^0$	-0.27763	-0.27763	0.0000002	-0.0000009
7	5	0.500000	6.99999	1s7h $^3\text{H}_4^0$	-0.27763	-0.27763	0.0000002	-0.0000009
7	6	0.500000	7.00000	1s7i $^3\text{I}_5$	-0.27763	-0.27762	-0.0000094	0.0000339
7	6	0.500000	7.00000	1s7i $^3\text{I}_6$	-0.27763	-0.27762	-0.0000094	0.0000339
7	6	0.500000	7.00000	1s7i $^3\text{I}_7$	-0.27763	-0.27762	-0.0000094	0.0000339
Avg.							0.0002768	-0.0001975

^a Radius of the inner electron 1 from Eq. (155).

^b Radius of the outer electron 2 from Eq. (150).

^c Classical quantum mechanical (CQM) calculated energy levels given by the electric energy (Eq. (102)).

^d Experimental NIST levels [19] with the ionization potential defined as zero.

^e (Theoretical-Experimental)/Experimental.

Table 7. Calculated and experimental energies of states of helium.

n	ℓ	r_1 (a_{He}) ^a	r_2 (a_{He}) ^b	Term Symbol	E_{ele} CQM He I Energy Levels ^c (eV)	NIST He I Energy Levels ^d (eV)	Difference CQM-NIST (eV)	Relative Difference ^e (CQM-NIST)
1	0	0.56699	0.566987	1s ² ¹ S	-24.58750	-24.58741	0.000092	-0.0000038
2	0	0.506514	1.42265	1s2s ³ S	-4.78116	-4.76777	-0.0133929	0.0028090
2	0	0.501820	1.71132	1s2s ¹ S	-3.97465	-3.97161	-0.0030416	0.0007658
2	1	0.500571	1.87921	1s2p ³ P ₂ ⁰	-3.61957	-3.6233	0.0037349	-0.0010308
2	1	0.500571	1.87921	1s2p ³ P ₁ ⁰	-3.61957	-3.62329	0.0037249	-0.0010280
2	1	0.500571	1.87921	1s2p ³ P ₀ ⁰	-3.61957	-3.62317	0.0036049	-0.0009949
2	1	0.499929	2.01873	1s2p ¹ P ⁰	-3.36941	-3.36936	-0.0000477	0.0000141
3	0	0.500850	2.42265	1s3s ³ S	-1.87176	-1.86892	-0.0028377	0.0015184
3	0	0.500302	2.71132	1s3s ¹ S	-1.67247	-1.66707	-0.0054014	0.0032401
3	1	0.500105	2.87921	1s3p ³ P ₂ ⁰	-1.57495	-1.58031	0.0053590	-0.0033911
3	1	0.500105	2.87921	1s3p ³ P ₁ ⁰	-1.57495	-1.58031	0.0053590	-0.0033911
3	1	0.500105	2.87921	1s3p ³ P ₀ ⁰	-1.57495	-1.58027	0.0053190	-0.0033659
3	2	0.500011	2.98598	1s3d ³ D ₃	-1.51863	-1.51373	-0.0049031	0.0032391
3	2	0.500011	2.98598	1s3d ³ D ₂	-1.51863	-1.51373	-0.0049031	0.0032391
3	2	0.500011	2.98598	1s3d ³ D ₁	-1.51863	-1.51373	-0.0049031	0.0032391
3	2	0.499999	3.00076	1s3d ¹ D	-1.51116	-1.51331	0.0021542	-0.0014235
3	1	0.499986	3.01873	1s3p ¹ P ⁰	-1.50216	-1.50036	-0.0017999	0.0011997
4	0	0.500225	3.42265	1s4s ³ S	-0.99366	-0.99342	-0.0002429	0.0002445
4	0	0.500088	3.71132	1s4s ¹ S	-0.91637	-0.91381	-0.0025636	0.0028054
4	1	0.500032	3.87921	1s4p ³ P ₂ ⁰	-0.87671	-0.87949	0.0027752	-0.0031555
4	1	0.500032	3.87921	1s4p ³ P ₁ ⁰	-0.87671	-0.87949	0.0027752	-0.0031555
4	1	0.500032	3.87921	1s4p ³ P ₀ ⁰	-0.87671	-0.87948	0.0027652	-0.0031442
4	2	0.500003	3.98598	1s4d ³ D ₃	-0.85323	-0.85129	-0.0019398	0.0022787
4	2	0.500003	3.98598	1s4d ³ D ₂	-0.85323	-0.85129	-0.0019398	0.0022787
4	2	0.500003	3.98598	1s4d ³ D ₁	-0.85323	-0.85129	-0.0019398	0.0022787
4	2	0.500000	4.00076	1s4d ¹ D	-0.85008	-0.85105	0.0009711	-0.0011411
4	3	0.500000	3.99857	1s4f ³ F ₃ ⁰	-0.85054	-0.85038	-0.0001638	0.0001926
4	3	0.500000	3.99857	1s4f ³ F ₄ ⁰	-0.85054	-0.85038	-0.0001638	0.0001926
4	3	0.500000	3.99857	1s4f ³ F ₂ ⁰	-0.85054	-0.85038	-0.0001638	0.0001926
4	3	0.500000	4.00000	1s4f ¹ F ⁰	-0.85024	-0.85037	0.0001300	-0.0001529
4	1	0.499995	4.01873	1s4p ¹ P ⁰	-0.84628	-0.84531	-0.0009676	0.0011446

5	0	0.500083	4.42265	1s5s ³ S	-0.61519	-0.61541	0.0002204	-0.0003582
5	0	0.500035	4.71132	1s5s ¹ S	-0.57750	-0.57617	-0.0013253	0.0023002
5	1	0.500013	4.87921	1s5p ³ P ₂ ⁰	-0.55762	-0.55916	0.0015352	-0.0027456
5	1	0.500013	4.87921	1s5p ³ P ₁ ⁰	-0.55762	-0.55916	0.0015352	-0.0027456
5	1	0.500013	4.87921	1s5p ³ P ₀ ⁰	-0.55762	-0.55915	0.0015252	-0.0027277
5	2	0.500001	4.98598	1s5d ³ D ₃	-0.54568	-0.54472	-0.0009633	0.0017685
5	2	0.500001	4.98598	1s5d ³ D ₂	-0.54568	-0.54472	-0.0009633	0.0017685
5	2	0.500001	4.98598	1s5d ³ D ₁	-0.54568	-0.54472	-0.0009633	0.0017685
5	2	0.500000	5.00076	1s5d ¹ D	-0.54407	-0.54458	0.0005089	-0.0009345
5	3	0.500000	4.99857	1s5f ³ F ₃ ⁰	-0.54431	-0.54423	-0.0000791	0.0001454
5	3	0.500000	4.99857	1s5f ³ F ₄ ⁰	-0.54431	-0.54423	-0.0000791	0.0001454
5	3	0.500000	4.99857	1s5f ³ F ₂ ⁰	-0.54431	-0.54423	-0.0000791	0.0001454
5	3	0.500000	5.00000	1s5f ¹ F ⁰	-0.54415	-0.54423	0.0000764	-0.0001404
5	4	0.500000	4.99988	1s5g ³ G ₄	-0.54417	-0.54417	0.0000029	-0.0000054
5	4	0.500000	4.99988	1s5g ³ G ₅	-0.54417	-0.54417	0.0000029	-0.0000054
5	4	0.500000	4.99988	1s5g ³ G ₃	-0.54417	-0.54417	0.0000029	-0.0000054
5	4	0.500000	5.00000	1s5g ¹ G	-0.54415	-0.54417	0.0000159	-0.0000293
5	1	0.499998	5.01873	1s5p ¹ P ⁰	-0.54212	-0.54158	-0.0005429	0.0010025
6	0	0.500038	5.42265	1s6s ³ S	-0.41812	-0.41838	0.0002621	-0.0006266
6	0	0.500016	5.71132	1s6s ¹ S	-0.39698	-0.39622	-0.0007644	0.0019291
6	1	0.500006	5.87921	1s6p ³ P ₂ ⁰	-0.38565	-0.38657	0.0009218	-0.0023845
6	1	0.500006	5.87921	1s6p ³ P ₁ ⁰	-0.38565	-0.38657	0.0009218	-0.0023845
6	1	0.500006	5.87921	1s6p ³ P ₀ ⁰	-0.38565	-0.38657	0.0009218	-0.0023845
6	2	0.500001	5.98598	1s6d ³ D ₃	-0.37877	-0.37822	-0.0005493	0.0014523
6	2	0.500001	5.98598	1s6d ³ D ₂	-0.37877	-0.37822	-0.0005493	0.0014523
6	2	0.500001	5.98598	1s6d ³ D ₁	-0.37877	-0.37822	-0.0005493	0.0014523
6	2	0.500000	6.00076	1s6d ¹ D	-0.37784	-0.37813	0.0002933	-0.0007757
6	3	0.500000	5.99857	1s6f ³ F ₃ ⁰	-0.37797	-0.37793	-0.0000444	0.0001176
6	3	0.500000	5.99857	1s6f ³ F ₄ ⁰	-0.37797	-0.37793	-0.0000444	0.0001176
6	3	0.500000	5.99857	1s6f ³ F ₂ ⁰	-0.37797	-0.37793	-0.0000444	0.0001176
6	3	0.500000	6.00000	1s6f ¹ F ⁰	-0.37788	-0.37793	0.0000456	-0.0001205
6	4	0.500000	5.99988	1s6g ³ G ₄	-0.37789	-0.37789	-0.0000023	0.0000060
6	4	0.500000	5.99988	1s6g ³ G ₅	-0.37789	-0.37789	-0.0000023	0.0000060
6	4	0.500000	5.99988	1s6g ³ G ₃	-0.37789	-0.37789	-0.0000023	0.0000060
6	4	0.500000	6.00000	1s6g ¹ G	-0.37788	-0.37789	0.0000053	-0.0000140
6	5	0.500000	5.99999	1s6h ³ H ₄ ⁰	-0.37789	-0.37788	-0.0000050	0.0000133
6	5	0.500000	5.99999	1s6h ³ H ₅ ⁰	-0.37789	-0.37788	-0.0000050	0.0000133
6	5	0.500000	5.99999	1s6h ³ H ₆ ⁰	-0.37789	-0.37788	-0.0000050	0.0000133

6	5	0.500000	6.00000	1s6h $^1H^0$	-0.37788	-0.37788	-0.0000045	0.0000119
6	1	0.499999	6.01873	1s6p $^1P^0$	-0.37671	-0.37638	-0.0003286	0.0008730
7	0	0.500019	6.42265	1s7s 3S	-0.30259	-0.30282	0.0002337	-0.0007718
7	0	0.500009	6.71132	1s7s 1S	-0.28957	-0.2891	-0.0004711	0.0016295
7	1	0.500003	6.87921	1s7p $^3P^0_2$	-0.28250	-0.28309	0.0005858	-0.0020692
7	1	0.500003	6.87921	1s7p $^3P^0_1$	-0.28250	-0.28309	0.0005858	-0.0020692
7	1	0.500003	6.87921	1s7p $^3P^0_0$	-0.28250	-0.28309	0.0005858	-0.0020692
7	2	0.500000	6.98598	1s7d 3D_3	-0.27819	-0.27784	-0.0003464	0.0012468
7	2	0.500000	6.98598	1s7d 3D_2	-0.27819	-0.27784	-0.0003464	0.0012468
7	2	0.500000	6.98598	1s7d 3D_1	-0.27819	-0.27784	-0.0003464	0.0012468
7	2	0.500000	7.00076	1s7d 1D	-0.27760	-0.27779	0.0001907	-0.0006864
7	3	0.500000	6.99857	1s7f $^3F^0_3$	-0.27769	-0.27766	-0.0000261	0.0000939
7	3	0.500000	6.99857	1s7f $^3F^0_4$	-0.27769	-0.27766	-0.0000261	0.0000939
7	3	0.500000	6.99857	1s7f $^3F^0_2$	-0.27769	-0.27766	-0.0000261	0.0000939
7	3	0.500000	7.00000	1s7f $^1F^0$	-0.27763	-0.27766	0.0000306	-0.0001102
7	4	0.500000	6.99988	1s7g 3G_4	-0.27763	-0.27763	-0.0000043	0.0000155
7	4	0.500000	6.99988	1s7g 3G_5	-0.27763	-0.27763	-0.0000043	0.0000155
7	4	0.500000	6.99988	1s7g 3G_3	-0.27763	-0.27763	-0.0000043	0.0000155
7	4	0.500000	7.00000	1s7g 1G	-0.27763	-0.27763	0.0000004	-0.0000016
7	5	0.500000	6.99999	1s7h $^3H^0_5$	-0.27763	-0.27763	0.0000002	-0.0000009
7	5	0.500000	6.99999	1s7h $^3H^0_6$	-0.27763	-0.27763	0.0000002	-0.0000009
7	5	0.500000	6.99999	1s7h $^3H^0_4$	-0.27763	-0.27763	0.0000002	-0.0000009
7	5	0.500000	7.00000	1s7h $^1H^0$	-0.27763	-0.27763	0.0000006	-0.0000021
7	6	0.500000	7.00000	1s7i 3I_5	-0.27763	-0.27762	-0.0000094	0.0000339
7	6	0.500000	7.00000	1s7i 3I_6	-0.27763	-0.27762	-0.0000094	0.0000339
7	6	0.500000	6.78349	1s7i 3I_7	-0.27763	-0.27762	-0.0000094	0.0000339
7	6	0.500000	7.00000	1s7i 1I	-0.27763	-0.27762	-0.0000094	0.0000338
7	1	0.500000	7.01873	1s7p $^1P^0$	-0.27689	-0.27667	-0.0002186	0.0007900
8	0	0.500011	7.42265	1s8s 3S	-0.22909	-0.22928	0.0001866	-0.0008139
8	0	0.500005	7.71132	1s8s 1S	-0.22052	-0.2202	-0.0003172	0.0014407
9	0	0.500007	8.42265	1s9s 3S	-0.17946	-0.17961	0.0001489	-0.0008291
9	0	0.500003	8.71132	1s9s 1S	-0.17351	-0.1733	-0.0002141	0.0012355
10	0	0.500004	9.42265	1s10s 3S	-0.14437	-0.1445	0.0001262	-0.0008732
10	0	0.500002	9.71132	1s10s 1S	-0.14008	-0.13992	-0.0001622	0.0011594
11	0	0.500003	10.42265	1s11s 3S	-0.11866	-0.11876	0.0001037	-0.0008734
11	0	0.500001	10.71132	1s11s 1S	-0.11546	-0.11534	-0.0001184	0.0010268
					Avg.		-0.0004341	0.0000385

^a Radius of the inner electron 1 of singlet excited states with $\ell = 0$ from Eq. (119); triplet excited states with $\ell = 0$ from Eq. (126); singlet excited states with $\ell \neq 0$ from Eq. (146) for $\ell = 1$ or $\ell = 2$ and Eq. (147) for

- $\ell = 3$, and Eq. (148) for $\ell = 4, 5, 6, \dots$; triplet excited states with $\ell \neq 0$ from Eq. (155), and $1s^2\ ^1S$ from Eq. (62).
- ^b Radius of the outer electron 2 of singlet excited states with $\ell = 0$ from Eq. (101); triplet excited states with $\ell = 0$ from Eq. (121); singlet excited states with $\ell \neq 0$ from Eq. (139); triplet excited states with $\ell \neq 0$ from Eq. (150), and $1s^2\ ^1S$ from Eq. (62).
- ^e Classical quantum mechanical (CQM) calculated excited-state energy levels given by the electric energy (Eq. (102)) and the energy level of $1s^2\ ^1S$ is given by Eqs. (63-65).
- ^d Experimental NIST levels [19] with the ionization potential defined as zero.
- ^e (Theoretical-Experimental)/Experimental.

Table 8. Calculated spin-orbital energies of He I singlet excited states with $\ell = 1$ as a function of the radius of the outer electron.

n	r_2 (a_{He}) ^a	Term Symbol	$E_{s/o}$ spin-orbital coupling ^b (eV)
2	2.01873	1s2p ¹ P ⁰	0.0000439
3	3.01873	1s3p ¹ P ⁰	0.0000131
4	4.01873	1s4p ¹ P ⁰	0.0000056
5	5.01873	1s5p ¹ P ⁰	0.0000029
6	6.01873	1s6p ¹ P ⁰	0.0000017
7	7.01873	1s7p ¹ P ⁰	0.0000010

^a Radius of the outer electron 2 from Eq. (139).

^b The spin-orbital coupling energy of electron 2 from Eq. (156) using r_2 from Eq. (139).

Figure 1. The orbitsphere is a two dimensional spherical shell of zero thickness with the Bohr radius of the hydrogen atom, $r = a_H$.

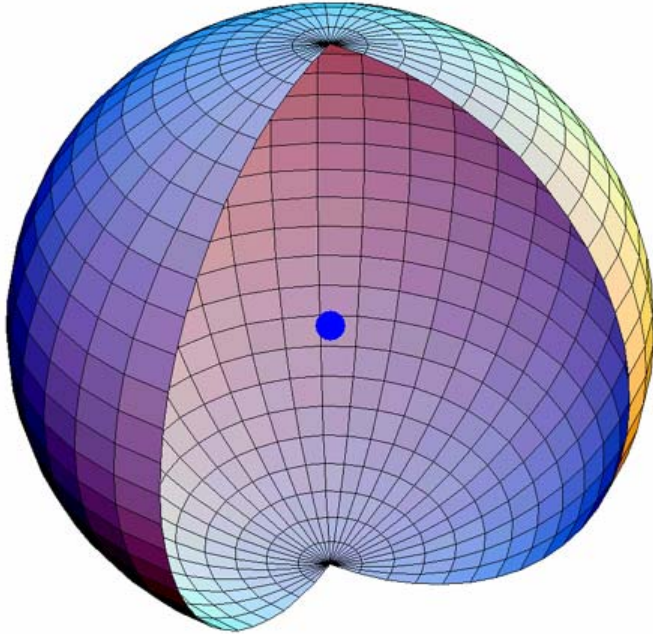


Figure 2. The current pattern of the orbitsphere from the perspective of looking along the z-axis. The current and charge density are confined to two dimensions at $r_n = nr_1$. The corresponding charge density function is uniform.

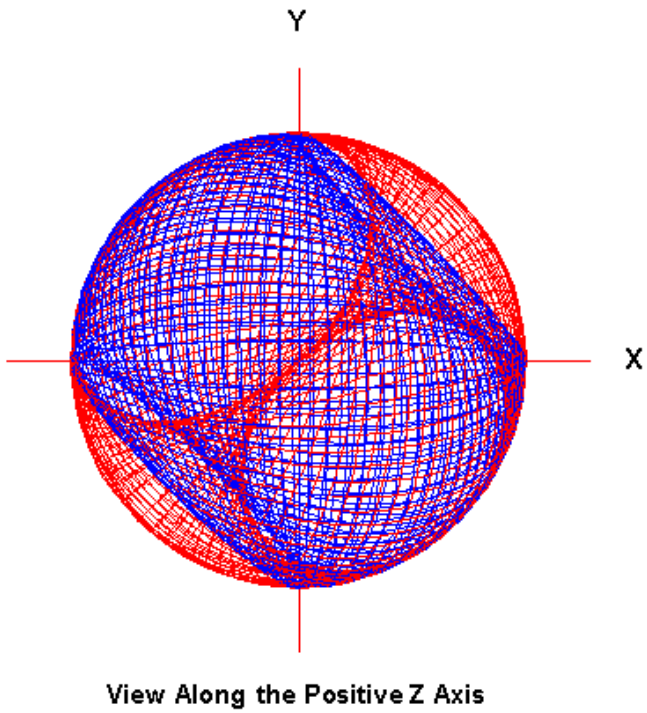


Figure 3. The orbital function modulates the constant (spin) function (shown for $t = 0$; three-dimensional view).

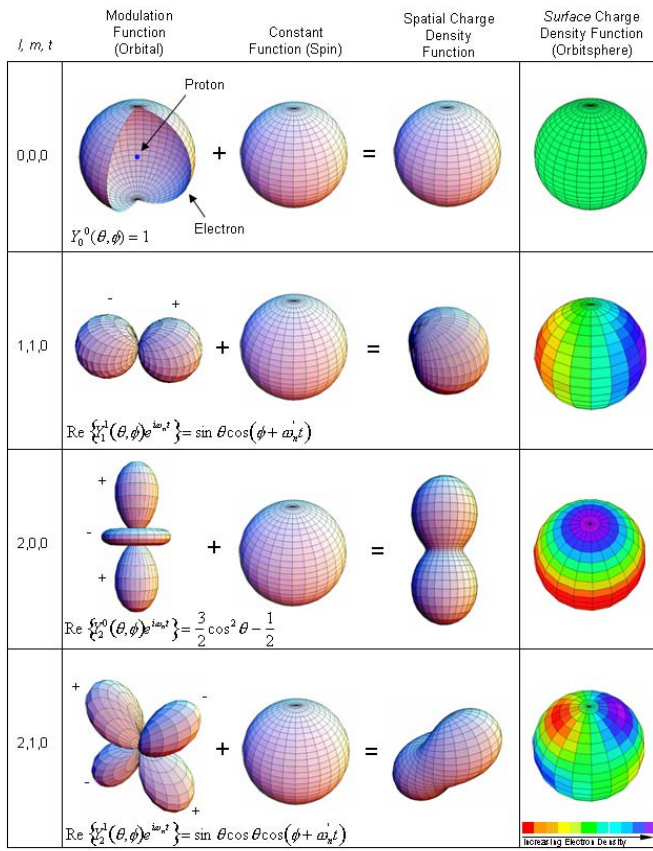


Figure 4. The normalized radius as a function of the velocity due to relativistic contraction.

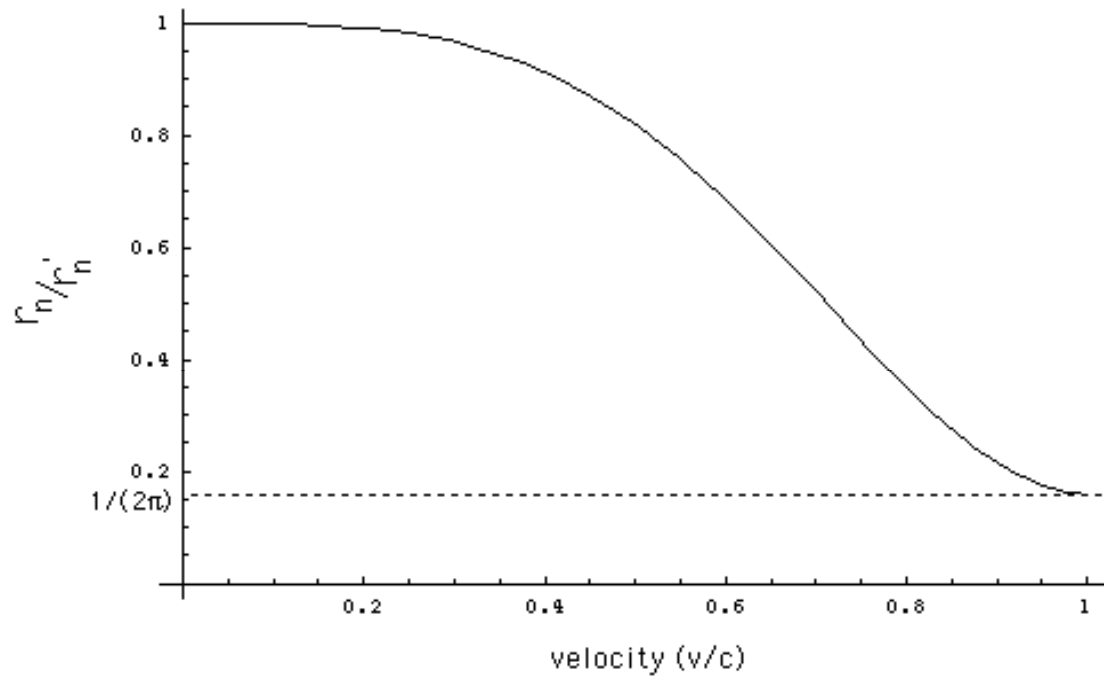


Figure 5. The magnetic field of an electron orbitsphere (z-axis defined as the vertical axis).

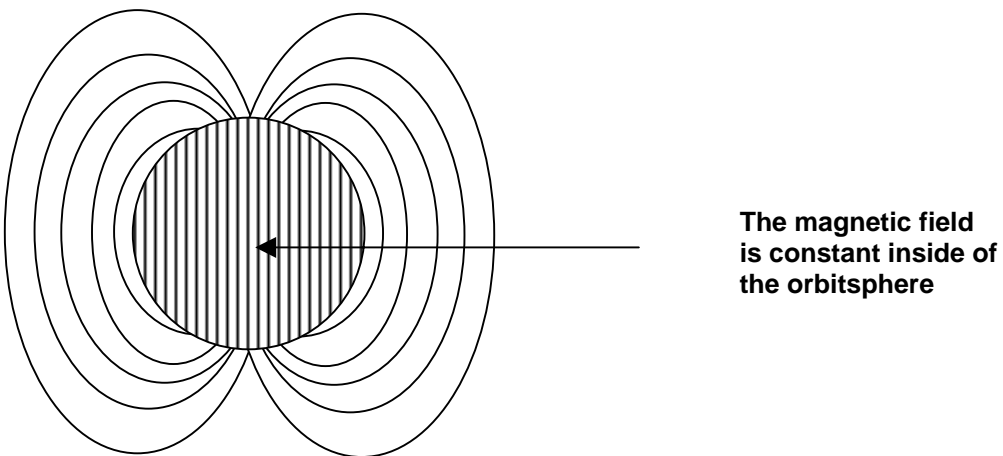


Figure 6. The experimental results of Bromberg [45], the extrapolated experimental data of Hughes [45], the small angle data of Geiger [46], and the semiexperimental results of Lassetre [45] for the elastic differential cross section for the elastic scattering of electrons by helium atoms and the elastic differential cross section as a function of angle numerically calculated by Khare [45] using the first Born approximation and first-order exchange approximation.

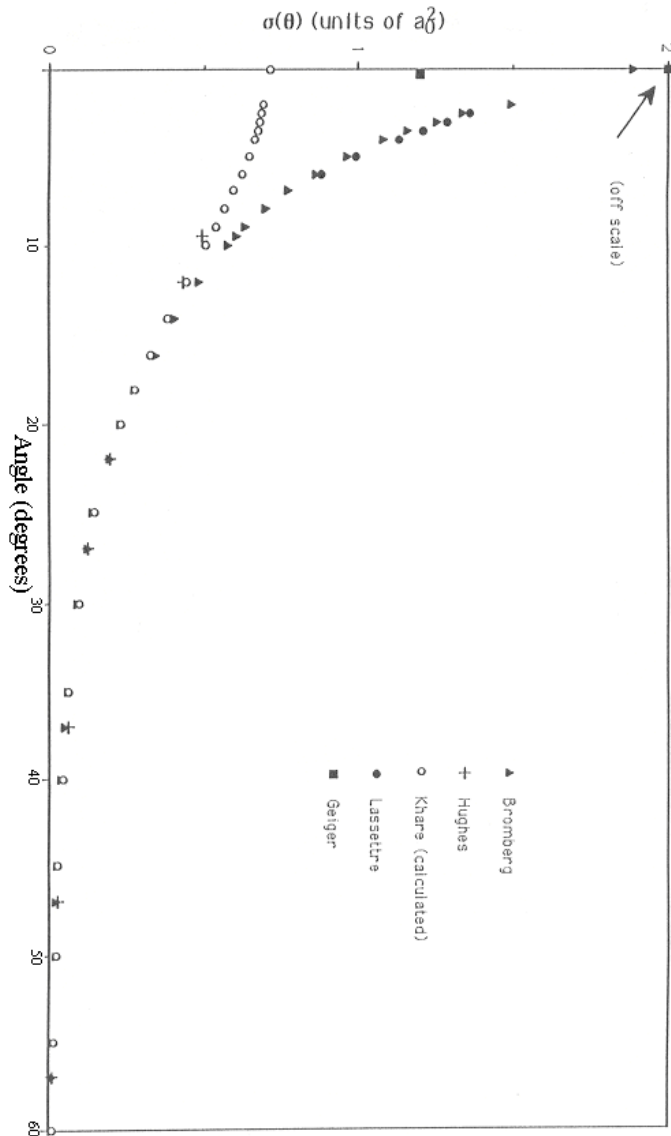


Figure 7. The closed form function (Eqs. (90) and (91)) for the elastic differential cross section for the elastic scattering of electrons by helium atoms. The scattering amplitude function, $F(s)$ (Eq. (89)), is shown as an insert.

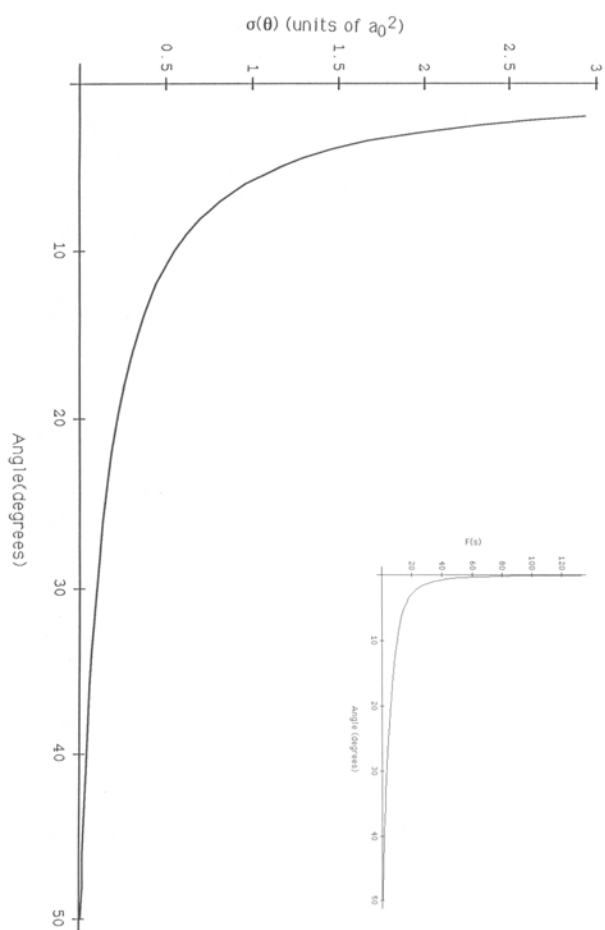


Figure 8. A plot of the predicted and experimental energies of levels assigned by NIST [19].

